DETECTION AND CLASSIFICATION OF QRS COMPLEXES FROM THE ECG RECORDINGS

A THESIS SUBMITTED TO
THE GRADUATE SCHOOL OF NATURAL AND APPLIED SCIENCES
OF
MIDDLE EAST TECHNICAL UNIVERSITY

BY

BENGİ KOÇ

IN PARTIAL FULFILLMENT OF THE REQUIREMENTS
FOR
THE DEGREE OF MASTER OF SCIENCE
IN
ELECTRICAL AND ELECTRONICS ENGINEERING

DECEMBER 2008

Approval of the thesis:

DETECTION AND CLASSIFICATION OF QRS COMPLEXES FROM THE ECG RECORDINGS

submitted by **BENGİ KOÇ** in partial fulfillment of the requirements for the degree of **Master of Science in Electrical and Electronics Engineering Department, Middle East Technical University** by,

Prof. Dr. Canan Özgen
Dean, Graduate School of **Natural and Applied Sciences** _____

Prof. Dr. İsmet Erkmen
Head of Department, **Electrical and Electronics Engineering** _____

Assist. Prof. Dr. Yeşim Serinağaoğlu Doğrusöz
Supervisor, **Electrical and Electronics Engineering Dept., METU** _____

Examining Committee Members

Prof. Dr. Nevzat Güneri Gençer
Electrical and Electronics Engineering Dept., METU _____

Assist. Prof. Dr. Yeşim Serinağaoğlu Doğrusöz
Electrical and Electronics Engineering Dept., METU _____

Prof. Dr. Murat Eyüboğlu
Electrical and Electronics Engineering Dept., METU _____

Assoc. Prof. Dr. Tolga Çiloğlu
Electrical and Electronics Engineering Dept., METU _____

Dr. Özlem Birgül
Chief Researcher, TÜBİTAK _____

Date: 16 December 2008

I hereby declare that all information in this document has been obtained and presented in accordance with academic rules and ethical conduct. I also declare that, as required by these rules and conduct, I have fully cited and referenced all material and results that are not original to this work.

Name, Last name: Bengi KOÇ

Signature :

ABSTRACT

DETECTION AND CLASSIFICATION OF QRS COMPLEXES FROM THE ECG RECORDINGS

Koç, Bengi

M.S., Department of Electrical and Electronics Engineering

Supervisor: Assist. Prof. Dr. Yeşim Serinağaoğlu Doğrusöz

December 2008, 96 pages

Electrocardiography (ECG) is the most important noninvasive tool used for diagnosing heart diseases. An ECG interpretation program can help the physician state the diagnosis correctly and take the corrective action. Detection of the QRS complexes from the ECG signal is usually the first step for an interpretation tool. The main goal in this thesis was to develop robust and high performance QRS detection algorithms, and using the results of the QRS detection step, to classify these beats according to their different pathologies. In order to evaluate the performances, these algorithms were tested and compared in Massachusetts Institute of Technology Beth Israel Hospital (MIT-BIH) database, which was developed for research in cardiac electrophysiology.

In this thesis, four promising QRS detection methods were taken from literature and implemented: a derivative based method (Method I), a digital filter based method (Method II), Tompkin's method that utilizes the morphological features of the ECG signal (Method III) and a neural network based QRS detection method (Method IV). Overall sensitivity and positive predictivity values above 99% are achieved with

each method, which are compatible with the results reported in literature. Method III has the best overall performance among the others with a sensitivity of 99.93% and a positive predictivity of 100.00%.

Based on the detected QRS complexes, some features were extracted and classification of some beat types were performed. In order to classify the detected beats, three methods were taken from literature and implemented in this thesis: a Kth nearest neighbor rule based method (Method I), a neural network based method (Method II) and a rule based method (Method III). Overall results of Method I and Method II have sensitivity values above 92.96%. These findings are also compatible with those reported in the related literature. The classification made by the rule based approach, Method III, did not coincide well with the annotations provided in the MIT-BIH database. The best results were achieved by Method II with the overall sensitivity value of 95.24%.

Keywords: Electrocardiography, ECG, QRS detection, feature extraction, classification

ÖZ

ECG SİNYALLERİNDEN QRS KOMPLEKS BULMA VE SINIFLANDIRMA

Koç, Bengi

Yüksek Lisans, Elektrik Elektronik Mühendisliği Bölümü

Tez Yöneticisi : Yrd. Doç. Dr. Yeşim Serinağaoğlu Doğrusöz

Aralık 2008, 96 sayfa

Elektrokardiyografi kalp rahatsızlıkları teşhisinde kullanılan müdahalesiz, en önemli yöntemdir. EKG yorumlama programları doktorlara doğru teşhisi koyup, gereğini yapabilmeleri için yardımcı olmaktadırlar. Yorumlama programlarında ilk aşama genellikle atımlardaki QRS komplekslerini bulmaktır. Bu tezin ana amacı, sağlam ve yüksek performanslı QRS komplekslerini bulma algoritmaları geliştirmek ve bulunan QRS komplekslerini kullanarak, atımları patolojilerine göre sınıflandırmaktır. Performansların değerlendirilmesi için, bu algoritmalar, kalp elektrofizyolojisi araştırmaları için geliştirilmiş olan "Massachusetts Institute of Technology Beth Israel Hospital (MIT-BIH) " veri tabanında test edilip, sonuçları karşılaştırılmıştır.

Bu tezde, literatürden umut verici dört algoritma seçilerek uygulanmıştır: türeve bağlı bir metot (Metot I), sayısal filtre metodu (Metot II), EKG sinyallerinin biçimsel özelliklerine dayalı Tompkin'in metodu (Metot III), ve yapay sinir ağı tabanlı QRS bulma metodu (Metot IV). Her bir metodun duyarlılık ve pozitif kestirim değerleri, toplamda, literatürde belirtilen değerlerle uyumlu olarak, %99'un üzerinde bulunmuştur. Metot III, %99.93 duyarlılık ve %100.00 pozitif kestirim

değerleri ile diğerleri arasında toplamda en iyi performansı göstermiştir.

Bulunan QRS komplekslerinde bazı öznitelikler çıkartılıp, bunlara göre bazı atım tiplerinin sınıflandırması yapılmıştır. Bulunan atımların sınıflandırması için bu tezde, literatürden üç metot alınarak uygulanmıştır: K. en yakın komşu metodu (Metot I), sinir ağları tabanlı bir metot (Metot II), ve kural tabanlı bir metot (Metot III). Metot I ve Metot II'nin duyarlılık değerleri %92.96'nın üzerinde bulunmuştur. Bulunan bu değerler de literatürde belirtilen değerlerle uyumludur. Kural tabanlı sınıflandırma metodu (Metot III) sonuçları, MIT-BIH veri tabanı anotasyonları ile çok uyumlu bulunmamıştır. Metot II, %95.24 duyarlılık değeri ile en iyi sonuçları vermiştir.

Anahtar Kelimeler: Elektrokardiyografi, EKG, QRS bulma, öznitelik çıkarma, sınıflandırma

ACKNOWLEDGMENTS

I would like to express my deepest gratitude to my supervisor Asst. Prof. Dr. Yeşim SERİNAĞAOĞLU DOĞRUSÖZ for her guidance, encouragements, advice, criticism, insight and patience throughout the research.

I would like to thank to Prof. Dr. Nazım ARSLAN for his technical assistance and guidance in medical aspects of this thesis.

I would like to thank to Onur DEMİRKOL and Mehmet YILMAZTÜRK for their useful discussions and Funda KÜREKSİZ for helping me in thesis format.

I would specially like to express my thanks to my family and my friends for their endless love, support and existence in my life.

To my parents and my brother

TABLE OF CONTENTS

LIST OF TABLES

TABLES

LIST OF FIGURES

FIGURES

LIST OF ABBREVIATIONS

Acronyms

AHA	American Heart Association
ANN	Artificial Neural Network
AV node	Atrioventricular node
CI	Computational Intelligence
CVD	Cardiovascular Diseases
CWT	Continuous Wavelet Transform
ECG	Electrocardiography
EMG	Electromyogram
F	Fusion of ventricular and normal beat
FIR	Finite Impulse Response
GUI	Graphical User Interface
HOS	Higher Order Statistics
IIR	Infinite Impulse Response
LBBB	Left Bundle Branch Block
LMS	Least Mean Squares
LVQ	Learning Vector Quantization

METU	Middle East Technical University
MI	Myocardial Infraction
MIT-BIH	Massachusetts Institute of Technology Beth Israel Hospital
MLP	Multilayer Perceptron
ms.	millisecond
PDA	Personnel Digital Assistant
PVC	Premature Ventricular Contraction
RBBB	Right Bundle Branch Block
RBF	Radial Basis Function
SA node	Sinoatrial node
SNR	Signal to Noise Ratio
SOM	Self Organizing Map
VEB	Ventricular Ectopic Beat
WPW syndrome	Wolff-Parkinson-White syndrome
WT	Wavelet Transform

CHAPTER 1

INTRODUCTION

Electrocardiography (ECG) is a graphical representation of potential differences between points on the body surface versus time and it is the most important noninvasive tool used for diagnosing the heart disease and guiding the therapy at both in-hospital and out-hospital applications.

Applications of ECG interpretation programs are usually for long-term monitoring purposes such as at the intensive-care units (ICU) in hospitals, ambulatory usages, and battery powered monitoring systems.

ICUs are for patients requiring special medical care. ICU display many parameters such as ECG, blood pressure, oxygen level in blood etc. When an abnormality exists, physicians working at the ICU must take immediate decisions that are usually very important for the patient life. An ECG interpretation program can help the physician to state the diagnosis correctly and take the corrective action.

Similar to ICUs, for ambulatory applications, physician's immediate decision and correct action are needed and ECG interpretation programs are helpful for that.

Battery powered compact size ECG recordings (Holter recording) and interpretation tools allow long term monitoring of patients outside hospitals without distorting the regular life of the patient allowing the transient aspects monitoring of heart electrical activity. By extracting the abnormal ECG complex within thousands of beats and suggesting the diagnosis, home monitoring ECG interpretation programs are cost effective and make the patient life comfortable compared to hospital monitoring.

ECG signal interpretation is an extensive area of research, but the basic steps are prefiltering, QRS detection, feature extraction and classification stages as illustrated

in Figure 1.1. Prefiltering stage is the digital filtering stage used to suppress artifacts such as baseline drift and in-coupling noise. The second stage is detection of the QRS complexes, which is the most important and characteristic feature generated by the depolarization wave passing through the ventricles. The third stage, which is a very extensive area of research, consists of finding the optimal set of features that maximize the classification performance in the last stage. In this stage other waves that constitute an ECG signal such as P, and T waves and the features depending on this waves such as PR interval and ST segment elevation or some other features such as QRS complex area, QRS complex maximum amplitude, QRS complex width and RR interval etc can be extracted. Finally in the last stage, classification of detected QRS beats according to extracted features is performed.

The main goal in this thesis is to develop robust and high performance QRS detection algorithms, and using the results of the QRS detection step, to classify these beats according to their different pathologies.

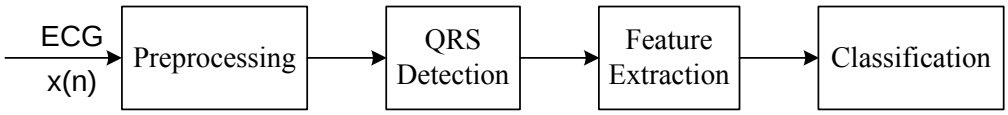

Figure 1.1 Common structure of ECG interpretation

1.1 Objectives of the Thesis

This thesis aims to provide a first step to the development of an extensive ECG interpretation tool. Towards that end, first the QRS beats are detected from the ECG recordings, then using these detected QRS waveforms and features derived from the properties of these QRS waveforms are used to classify the QRS beats. The steps of this work can be summarized as follows:

1) QRS detection step:

a. Implement a prefiltering step to suppress artifacts from the ECG signal to enhance the performances of the QRS detection algorithms

b. Implement four promising QRS detection algorithms taken from literature:

    i. a derivative based method (Method I),

    ii. a digital filter based method (Method II),

    iii. Tompkin's method that utilizes the morphological features of the ECG signal (Method III)

    iv. a neural network based QRS detection method (Method IV).

c. Evaluate the performances of these QRS detection algorithms by testing and comparing the results in Massachusetts Institute of Technology Beth Israel Hospital (MIT-BIH) database, which was developed for research in cardiac electro-physiology. The comparisons are made

    i. between the results obtained by each method in this thesis,

    ii. the results of this thesis and those obtained in similar studies in literature.

2) QRS beat classification step:

a. Define and extract features from the ECG signals using the results of the QRS detection step obtained from the QRS detection algorithm with the best performance

b. Implement three promising algorithms taken from literature to classify the detected QRS beats according to their different pathologies:

    i. K-th nearest neighbour rule (Classification Method I).

ii. Artificial neural networks (Classification Method II),

iii. A rule based classification (Classification Method III).

With the first two classification methods, only normal beats and premature ventricular contraction (PVC) beats are classified. With the third method, beats with various morphologies are classified.

c. Evaluate the performances of these classification algorithms again by using the MIT-BIH database. Similar to the QRS detection step, the comparisons are made

i. between the results obtained by each method in this thesis,

ii. the results of this thesis and those obtained in similar studies in literature.

3) Prepare a Graphical User Interface (GUI) for the implementation of the above steps of this thesis.

1.2 Outline of the Thesis

In Chapter 1, introduction to the subject matter is given. Then the objective of this thesis is stated. Finally, outline of the thesis report is presented.

In Chapter 2, background information is provided.

In Chapter 3, methods of the developed algorithms are explained.

In Chapter 4, performance evaluation of the algorithms are provided.

In Chapter 5, a brief summary on the performed study is given. This chapter also contains some concluding remarks and recommendations for future works.

In Appendix A, graphical user interface (GUI) developed for these algorithms is explained.

CHAPTER 2

BACKGROUND

This chapter starts with brief explanation of medical background, followed by literature survey on QRS detection, feature extraction and classification. Then continues with background information on performance evaluation and ECG databases.

2.1 Medical Background

In this part anatomy, physiology and electrical activity of the heart are briefly explained based on the information provided in [1] and [2].

2.1.1 Anatomy and Physiology of the Heart

Location of the heart is in thorax; between the lungs behind the sternum and the diaphragm as illustrated in Figure 2.1

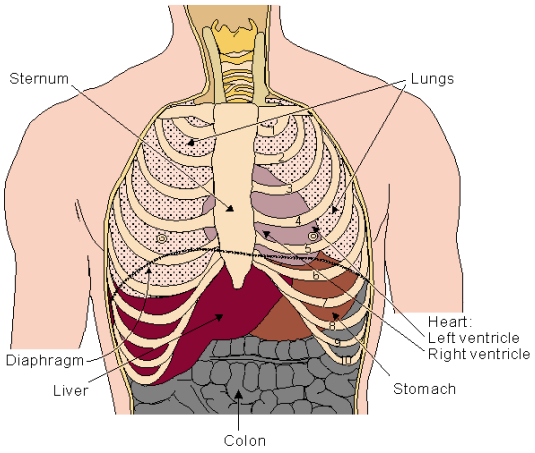

Figure 2.1 Location of the heart [1]

The heart walls are composed of mainly cardiac muscle, called myocardium and some striations. Compartments of the heart are right atria, left atria, right ventricle and left ventricle. The anatomy of the heart and related vessels are illustrated in Figure 2.2.

Valves of the heart are tricuspid (between right atrium and ventricle), mitral (between left atrium and ventricle), pulmonary (between right ventricle and pulmonary artery) and aortic (between left ventricle and aorta). Deoxygenated blood returned from the systemic circulation enters right atrium and through tricuspid valve goes to right ventricle. It is pumped out from right ventricle to lungs through pulmonary valve. From the lungs oxygenated blood enters to left atrium, through mitral valve goes to left ventricle. And then, oxygenated blood is pumped to whole body through aorta via the aortic valve.

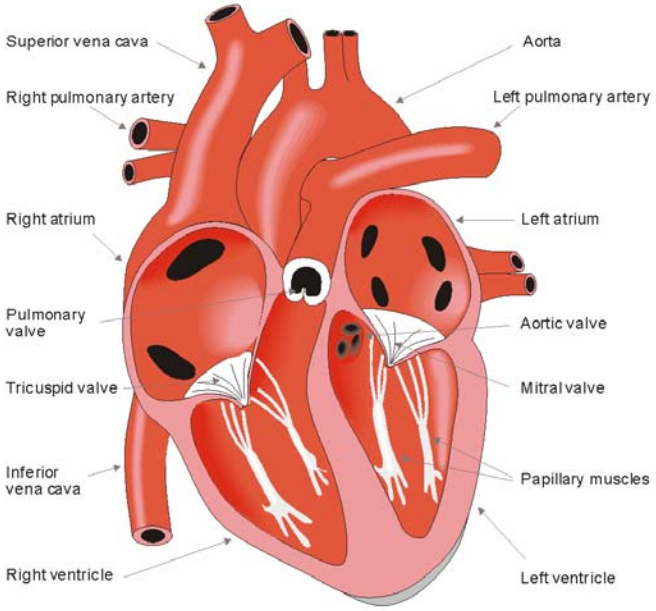

Figure 2.2 Anatomy of the hearth and related vessels [1]

2.1.2 Electrical Activity of the Heart

Mechanism of the electric activation in a heart muscle cell, myocyte, is the same as in a nerve cell.

The distribution of ions across the cell membrane creates a potential difference across the membrane of the cell. This potential difference is called the transmembrane potential. The transmembrane becomes charged and its potential increases during impulse propagation with action potential impulses. An action potential is a carrier of the information providing the control and coordination of organs like heart. An action potential is a wave of electrical discharge that propagates along the membrane of a cell. Depolarization increases the membrane potential and repolarization decreases the membrane potential so that membrane potential returns to its resting potential, as shown in Figure 2.3 [3].

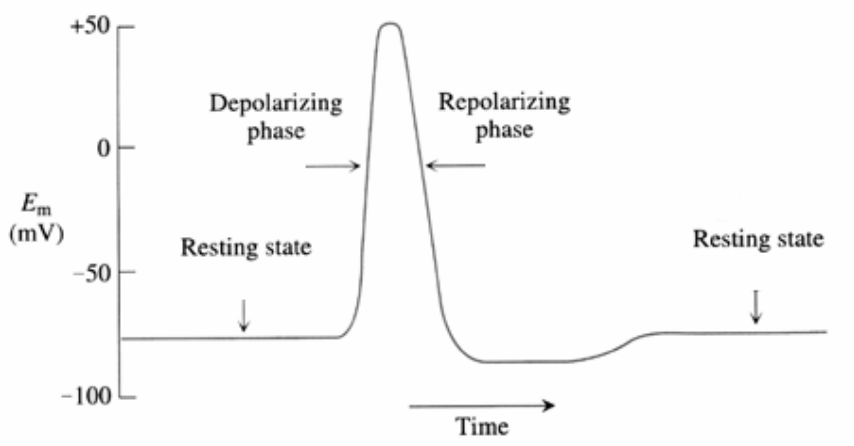

Figure 2.3 Depolarization, repolarization and the resting phases of action potential [3].

In muscle cells, inflow of sodium ions across the cell membrane creates action potential with amplitude about 100 mV and duration is about 300 ms.

Electrical activation between cardiac muscle cells propagates and mechanical contraction follows the electrical activation.

Sinoatrial node (SA node) consisting of specialized, self-excitatory, pacemaker muscle cells is located at superior vena cava in right atrium. These pacemaker cells stimulate electrical activation about 70 times in a minute in a normal heart. Stimulated

action potentials propagate through the atria but not to the ventricles since there is a nonconducting barrier in the boundary between the atria and ventricles.

AV node is located at the boundary between atria and ventricles. Similar to SA node, AV node consists of specialized, self-excitatory, pacemaker muscle cells stimulating electrical activation about 50 times in a minute. But if the AV node is on the path of an electrical activity having higher frequency, the intrinsic frequency of the AV node does not appear. Since at normal conditions, the action potential stimulated by SA node pass through AV node and intrinsic frequency of AV node is about 50 times/min, which is lower than SA node frequency which is of 70 times/min, SA node behaves just as a normal conducting path from atria to ventricles.

Action potential propagation from AV node to ventricles is through a specialized bundle system, called bundle of His and its branches called Purkinje fibers.

Critical points of the above process are as illustrated in Figure 2.4.

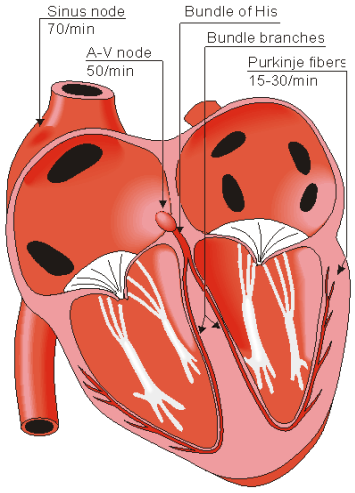

Figure 2.4 Heart conduction system [1]

2.1.3 ECG Waveform

The waves of depolarization that propagate through the heart during each cardiac cycle create electrical impulses basically composed of P,QRS and T waves as

depicted in Figure 2.5. These impulses propagate through various body fluids such as blood, up to body's surface and then surface electrodes if there exist. These signals are then captured by an electrocardiograph, which amplifies, filters and records the signal resulting in consecutive waveforms called as the ECG [2].

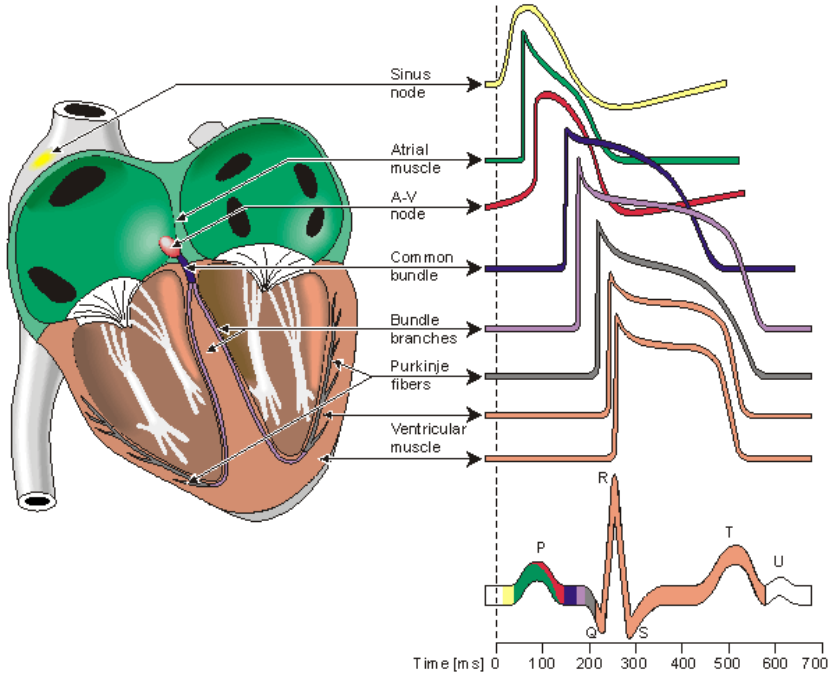

Figure 2.5 Heart electrophysiology [1]

As depicted in Figure 2.6, the main features of the ECG waveform that carry important information concerning cardiac heart are as follows:

- P wave
- QRS wave
- T wave
- QRS segment intervals

These features are described in the following section.

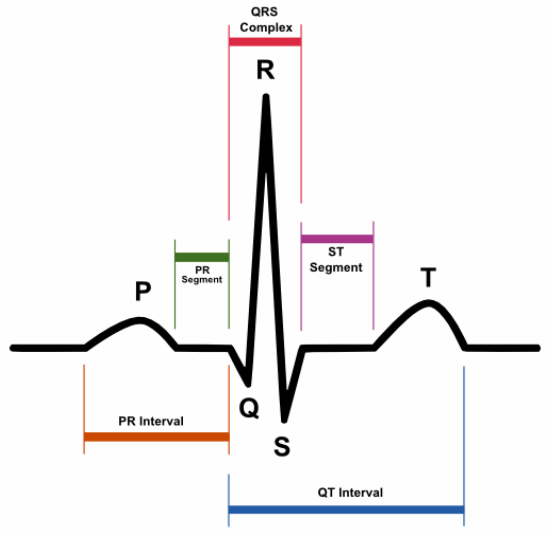

Figure 2.6 QRS complex showing the sinus rhythm regions [2]

2.1.3.1 P Wave

The P wave is a result of electrical activity originating from atrial contraction (systole). In cardiovascular diseases (CVDs), the P wave can appear in an abnormal shape as seen, for example in Figure 2.7. Abnormality in P wave can be a sign of various heart diseases such as negative P wave is an indication of abnormality in polarization direction of atria which means that the origin of the peacemaker signal is not the SA node, but could come from somewhere else such as the atrium or the AV node. Broadened or notch shape in P wave is an indication of delay in depolarization of the left atrium, which possibly arise from problems in conduction system. P waves exceeding 3 mm on the ECG trace, usually an indication of right atrial enlargement (P pulmonale). In some cases, the P wave is not apparent because of a junctional rhythm or SA block, whereas in some other cases it may be replaced by small oscillations or fibrillation waves (atrial flutter) [2].

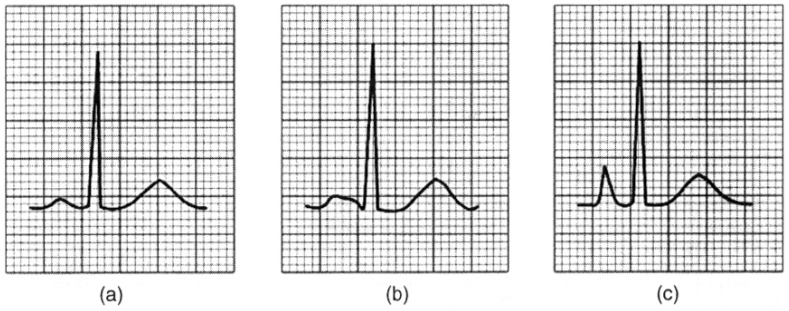

Figure 2.7.An example of various P-wave measurements from Lead II (a) Normal (b) broadened or notch, and (c) tall and peaked [2]

2.1.3.2 QRS complex

The QRS complex is due to ventricular contraction (systole) and the most important waveform reflecting electrical activity within the heart. It forms the basis of automatic detection of heart rate and also a starting point for classification and data compression algorithms [4]. The shape and occurrence QRS complex gives important information on the mechanical action of the heart giving with operation of each chamber.

The QRS complex is composed of the Q, R and S waves. Q wave is the first negative (downward) deflection. Followed the Q wave, R wave is the positive (upward) deflection. Any negative deflection following just after the R wave is named as the S wave. In some cases, two or more R waves can exist or R wave does not exist at all within one QRS complex as depicted in Figure 2.8.

The electrode/lead from which ECG signal is measured also affects the appearance of the wave. For example, from lead VI (right hand side of the heart), a large S wave is seen due to left ventricular forces passing away from the electrode. Healthy Q waves do not normally exceed 2 mm in amplitude or 0.03 s in width and abnormally large Q waves can be indication of myocardial infarction (MI). The QRS complex is usually not longer than 0.1 s and with average duration of 0.06-0.08s [2].

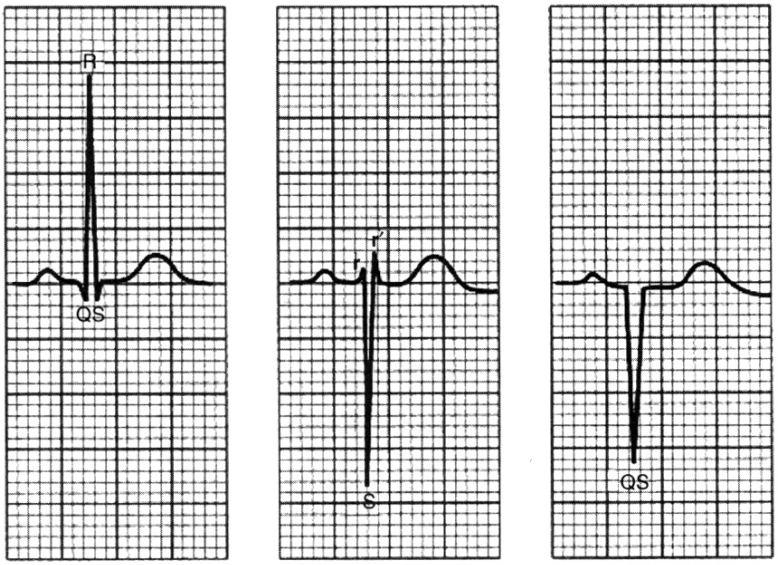

Figure 2.8 Various QRS complexes in the ECG [2]

2.1.3.3 T Wave

T wave is generated by the ventricles relax (diastole) after ventricular contraction. Unlike the Q and R waves, T wave is due to repolarization. T wave normally occurs for 0.25-0.35 s after ventricular depolarization. The lower heart chambers are electrically relaxing and preparing for their muscle contraction, during T wave. Atria repolarization is difficult to observe because it is masked by the larger QRS complex due to ventricular contraction. The T wave is in the same direction with the QRS complex because repolarization occurs in the direction opposite to depolarization. T waves are usually shorter than 5 mm in the standard leads. Abnormally tall T waves can be an indication of MI, whereas flattened T waves can be an indication of myxoedema and hypokalaemia. Slight T wave inversion can be due to hyperventillation and smoking however it is usually due to myocardial ischaemia, infarctions, ventricular hypertrophy, and bundle branch block [2].

2.1.3.4 QRS Segment Intervals

Both the shape and the time intervals of the waves are important in the evaluation of

cardiac health.

PQ interval is defined as the time interval between the beginning of the P wave and the onset of the QRS complex. But since the Q wave is often absent in this interval; the term PR interval is used representing the time between the onset on atrial contraction which is normally about 0.16 s [2].

If the heart tissue is scarred or inflamed, PR interval usually becomes longer as more time is needed for the depolarization wave to propagate through the atrial myocardium and the AV node. Shortened PR interval may be the indication of junctional tissue originated impulse or the Wolff-Parkinson-White syndrome [2].

The ST segment as depicted in Figure 2.9, is a very important interval in a way that various CVD is reflected to this segment. It is usually a leveled straight line between the QRS complex and the T wave. If the heart muscle is damaged or does not receive sufficient blood, some disturbances appears in ventricular repolarization causing ST segments to be elevated or depressed depending on the observed ECG lead. Concave upward ST segments over many cardiac cycles is an indication of pericarditis. Shape of ST segment depression is characteristic to pathologies which can indicate ventricular hypertophy, acute myocardial ischemia, and sinus tachycardia [2].

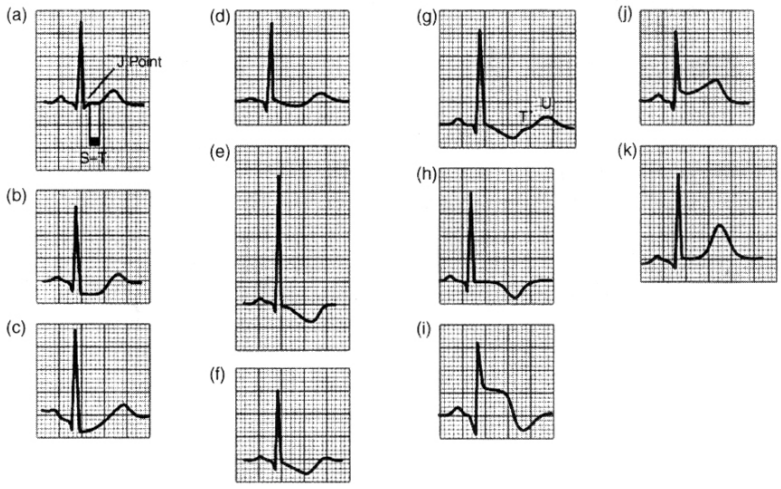

Figure 2.9 ST segments in the ECG [2]

QT interval, which is about 0.35 s., reflects the state of ventricular contractions. As heart rate increases, the duration of QT interval shortens. Although sometimes QT interval is difficult to measure, usually QT interval does not exceed half the time between the previous RR interval if the heart rate is between 60 and 90 beats/min. Longer QT intervals can be the indication of the risk of ventricular tachycardia or the presence of certain drugs like antidepressants. [2]

2.1.4 ECG Lead System

The voltages obtained during a normal ECG monitoring depend on the placement pf the recording electrodes (leads) on the body surface [2]. In order to achieve low contact impedance so that to maximize the ECG signal several lead placement and configurations are proposed for different purposes [5]. Among them three basic configurations are used in clinical applications. These are:

- Standard clinical ECG
- Vectorcardiogram (VCG)
- Monitoring ECG (1 or 2 leads)

Bipolar leads termed as I, II, and III are electrodes attached to the limbs. The potential difference is obtained by subtracting voltage of one lead from the voltage of another lead. For example for lead I, positive electrode is placed on the left arm and negative electrode is placed on the right arm. And the lead I potential is obtained by subtracting the right arm voltage from the left arm voltage [2].

The potential difference of the unipolar leads is obtained by subtracting voltage of positive lead from an indifferent voltage that is either ground or a small potential such as Wilson terminal, which is composed of the three limb lead electrodes [2].

Placement of 12 leads is depicted in Figure 2.10 and Table 2.1. An example of ECG waveforms that are obtained from these leads are depicted in Figure 2.11.

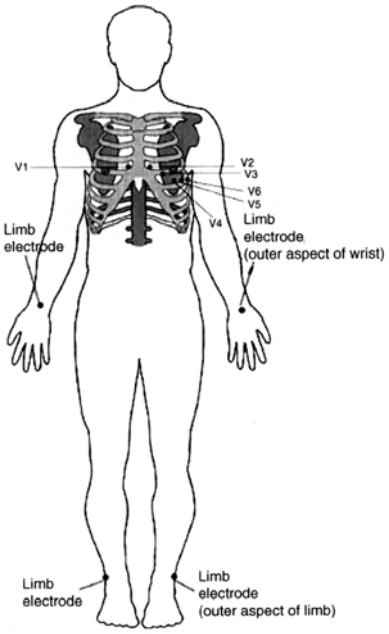

Figure 2.10 Placement of 12-Lead ECG [2]

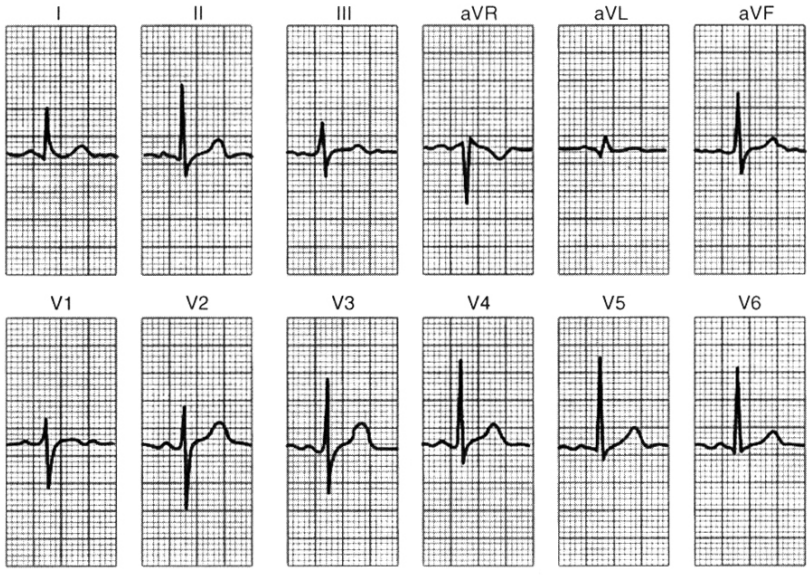

Figure 2.11 Example of ECG waveforms that are obtained from 12-Lead ECG [2]

Table 2.1 Placement of 12-Lead ECG [2]

Lead	Type	+ Electrode	- Electrode
I	Bipolar	Left arm	Right arm
II	Bipolar	Left foot	Right arm
III	Bipolar	Left foot	Left arm
V1	Unipolar	4^{th} intercoastal space to the right of	Ground
V2	Unipolar	4^{th} intercoastal space to the left of sternum	Ground
V3	Unipolar	Midway between V2 and V4	Ground
V4	Unipolar	5^{th} intercoastal space	Ground
V5	Unipolar	Left anterior axillary line on the same latitude as V4	Ground
V6	Unipolar	Left midaxillary line on the same latitude as V4	Ground
aVR	Unipolar	Right arm	Ground
aVL	Unipolar	Left arm	Ground
aVF	Unipolar	Left foot	Ground

Standard clinical ECG is implemented in hospital to a resting patient by using 12 leads (measured I, II, V1 to V6 and computed III, aVL, aVR and aVF).

In VCG, 3 orthogonal leads are used to obtain 3 dimensional vector model for the cardiac electrical activity.

Monitoring ECG, is implemented by using 1 or 2 leads to perform arrhythmia analysis in long term monitoring ICU, ambulatory or battery powered applications.

Since main objective in monitoring ECG applications is to recognize each heart beat and perform arrhythmia analysis, the leads at which R wave is most apparent are selected so that high signal to noise ratio is achieved. Since lead II has the highest R wave amplitude among the other leads in general, it is the first choice for monitoring applications. Second lead is considered as a backup source in case a malfunction such as loss of electrode occurs in lead II channel.

2.2 Prefiltering

Various sources of noise corrupt the ECG signal. The noise in recorded ECG may effect the interpretation of the recording and may lead an incorrect diagnosis [2]. Although some part of the noise is suppressed by hardware, there still exists some part of the noise in the recorded ECG. Therefore, prefiltering is necessary in order to attenuate artifacts before processing in the recorded ECG. The commonly encountered noises are described in the following sections [6].

Power line interference: The frequency content of power line interference is 50 or 60 Hz as the fundamental component with its harmonics. The amplitude of the power line interference may be up to %50 of peak to peak ECG signal amplitude as depicted in Figure 2.12 [6].

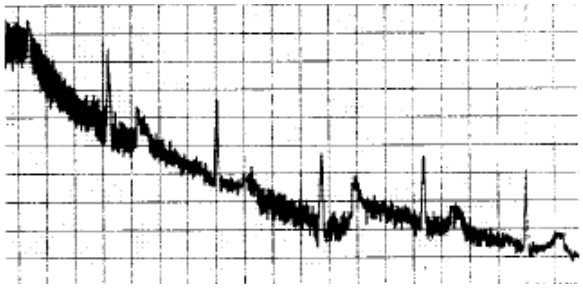

Figure 2.12 Power line interference and motion artifacts [6]

Electrode contact noise: As a result of contact loss between the electrode and skin, a transient step interference occurs called as electrode contact noise as depicted in Figure 2.13 [6].

Figure 2.13 Electrode contact noise [6]

Motion artifacts: Transient baseline changes occur which are called as motion artifacts as depicted in Figure 2.12 as a result of the changes in electrode-skin impedance with electrode motion [6].

Muscle contractions (EMG) artifacts:

Artificial milivolt-level potentials are generated due to muscle contractions. These artifacts are usually considered as zero mean Gaussian noise within DC to 10 kHz [6].

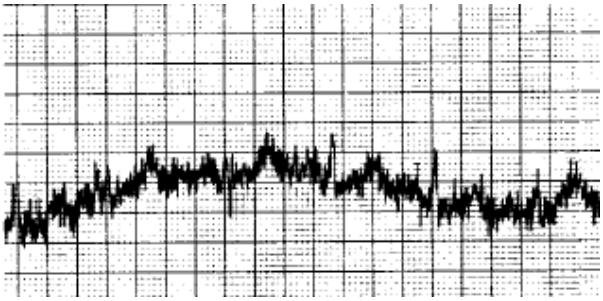

Figure 2.14 Respiration and EMG noise [6]

Baseline drift and ECG amplitude modulation with respiration: Respiration drifts the baseline of the ECG by adding a sinusoidal at the respiration frequency about 0.15 to 0.3 Hz as depicted in Figure 2.14 [6].

Electrosurgical Noise: ECG is destroyed if electrosurgical noise exists. Electrosurgical noise can be represented with a sinusoidal wave between 100 kHz to 1

MHz with amplitude in the order of % 200 of peak-to-peak ECG amplitude. Electrosurgical noise can not be filtered out since the sampling rate of ECG signal is in between 250 Hz to 1000 Hz which is below Nyquist rate which is not enough to prevent aliasing [6].

Conclusion: Preprocessing of ECG signals is necessary to suppress the various noise components and increase the signal to noise ratio (SNR) as much as possible. In general, cascade of high pass and low pass filtering which means band pass filtering with pass band covering 10 Hz to 25 Hz is used in order to noise reduction and extraction of characteristic features of QRS complex [4].

2.3 QRS Complex Detection

Among the several waveforms that compose an ECG signal, the most important and characteristic one is the QRS complex reflecting the electrical activity of the heart during ventricular contraction. Both the time of QRS complex occurrence and the shape of QRS complex provide important information about the current state of the heart such as determination of heart rate and forming the starting point of the interpretation programs. QRS complex characteristic shape is also used for ECG data compression algorithms. Therefore, QRS complex is the basis for ECG analysis algorithms.

Software QRS detection algorithms replaced hardware QRS detection algorithms for more than 35 years and after that many researches have been performed on software QRS detection [4]. In the early years computational load was the major drawback on software QRS detection but parallel to the developments in computer technology, computational load became less important and major objective became the detection performance of QRS complexes. However, the trend is now toward producing smaller and portable devices by employing PDA technology therefore accurate methods with less computational load became more important.

The review by [6] provides implementation of several QRS detection algorithms and

comparisons between them. Their test results showed that none of the algorithms was able to detect the QRS complexes without false positives for all the noise types at the highest noise levels. It is concluded that algorithms based on amplitude and slope have the best results for EMG captured ECG and an algorithm utilizing a digital filter had the best performance for the composite noise corrupted data.

A more recent review article, [4] provides approaches applied to QRS detection problem including derivative based algorithms, digital filters, artificial neural networks (ANN), genetic algorithms, wavelet transforms, filter banks and heuristic methods. Another review article, [7] outlines wavelet based algorithms used in ECG analysis.

As stated in [4], many of the publications' evaluation is not given, many of the publications' evaluation is not performed on standard databases or many of the publications' performance indices are not compatible (ie: sensitivity and positive predictability is not given). Therefore, the algorithms are not comparable effectively, although for many algorithms in the literature, sensitivities about %99 is claimed to be achieved. Additionally, only overall results are provided for detection rates, hiding the problems for individual records having pathological beats and noise corruption.

A review of mature QRS detection algorithms, which are proved to be successful, is given in the following sections.

2.3.1 Amplitude and Derivative Based Algorithms

The most fundamental algorithms in QRS detection are the ones based on amplitude and derivative of the ECG signal. Many algorithms in literature use first derivative, second derivative, or weighted combination of first and second derivatives. Differentiation is a way of high pass filtering allowing detection of QRS complex from its characteristic steep slope. QRS detection is achieved by comparing the feature obtained from derivative based algorithm, against a threshold. Signal-depended threshold is used in order to adapt to the varying signal characteristics.

Amplitude or first derivative peaks among over threshold samples are defined in order to locate the QRS complexes.

Let $x(n) = x(0)$, $x(1), \ldots x(n)$ be the discrete samples of an ECG signal. The parts of ECG signal at which the linear combinations of first derivative, $y'(n)$, and second derivative , $y''(n)$, calculated. Several implementations are:

$$y'(n) = x(n+1) - x(n) \tag{2.1}$$

$$y'(n) = x(n+1) - x(n-1) \tag{2.2}$$

$$y'(n) = 2x(n+2) - x(n+1) - x(n-1) - 2x(n-2) \tag{2.3}$$

$$y''(n) = x(n+2) - 2x(n) - x(n-2) \tag{2.4}$$

$$z(n) = 1.3\left|y'(n)\right| + 1.1\left|y''(n)\right| \tag{2.5}$$

After calculating these features, the parts (usually consecutive ones) that exceed an amplitude threshold are taken as a part of QRS complex. Usually signal dependent amplitude thresholds are defined for threshold to adapt the changing signal characteristics as much as possible. For example, an amplitude threshold, θ, is computed as a fraction of the maximum ECG signal amplitude as follows:

$$\theta = \gamma \max\left[x(n)\right] \tag{2.6}$$

where γ = 0.3, 0.4 have been widely used and maximum is determined from the current signal segment.

In order to exclude the non-QRS segments having QRS like feature values, some heuristic rules usually on the timing and the sign of the feature are applied. Therefore, number of false positives is decreased.

In a recent study performed by Arzeno, Deng and Poon [12], traditional Hamilton-

Tompkins algorithm [11] and a Hilbert transform based algorithm are implemented and compared. It is concluded that Hilbert transform based algorithm had accuracy of 99.13% sensitivity and 99.31% positive predictivity and Hamilton and Tompkins algorithm has the highest detection accuracy with 99.68% sensitivity and 99.63% positive predictivity.

Moraes, Freitas and Costa [14] developed a derivative based QRS detection algorithm allowing 2nd QRS detection channel to confirm or reject the results obtained from 1st QRS detection channel. This algorithm offers a sensitivity of 99.22% and 99.73%.

Amplitude and derivative based algorithms form the bases of QRS detection. Major principles have been described here. Further articles on amplitude and derivative based QRS detection include [2], [4], [5], [6], [8], [9], [10], [11], [12], [13], and [14].

2.3.2 Digital Filter Based Algorithms

Digital filters are widely applied for QRS detection. Bandpass filters are commonly used to enhance the waveform of interest and suppress the rest of the waveforms. A pioneer algorithm implemented by [6], ECG signal is filtered by two different low pass filters having different cut off frequencies. The difference between the filter outputs is the band pass filtered ECG signal having relatively high frequency components, QRS complex, enhanced and others suppressed. This band-passed filtered signal, $y2(n)$, is further processed by a nonlinear operation, which leads suppression of small values, and further enhancing QRS complex with the cost of smoothing the peaks of QRS complex.

$$y3(n) = y2(n)\left[\sum_{k=n-m}^{n+m} y2(k)\right]^2 \tag{2.7}$$

Multiplication of backward difference (MOBD) algorithm that Suppappola and Sun [15] proposed, is based on AND combination of adjacent magnitudes of derivatives.

$$z(n) = \prod_{k=0}^{N-1} \left| x(n-k) - x(n-k-1) \right| \tag{2.8}$$

A sign constraint is defined (2.9) in order to avoid noisy segments to make high feature signal. Threshold is selected to be depended on feature maximum z_{max}.

$$z(n) = 0 \text{ if } sign[x(n-k)] \neq sign[x(n-k-1)] \tag{2.9}$$

Some algorithms utilize other heuristic constraints to avoid the effects of noise.

QRS complexes are detected comparing the amplitudes in the band pass filtered signal with a variable v, where v is the maximum sample value of the recent segment. If, for example, ECG samples in the following segment are below v/2, a peak is detected. Some algorithms utilizes [16] recursive and nonrecursive median filters assuming that the QRS complex occur within the pass band of the filters. These filters are:

$$y(n) = median[y(n-m),....., y(n-1), x(n), x(n+1),...., x(n+m)] \tag{2.10}$$

$$y(n) = median[x(n-m),....., x(n-1), x(n), x(n+1),...., x(n+m)] \tag{2.11}$$

Adaptive filters [17] have also been utilized with the objective of modeling the ECG signal as a superposition based on the past signal values:

$$y(n) = \sum_{k=1}^{p} a_k(n) x(n-k) \tag{2.12}$$

where a_k are time variant coefficients adapting according to input signal statistics. A midprediction filter [18] has also been utilized based on the current signal segment:

$$y(n) = \sum_{k=-p}^{p} a_k(n) x(n-k) \tag{2.13}$$

Coefficients are obtained by using standard adaptation rules such as the least mean squares (LMS) algorithm.

Major principles of digital filter based QRS detection algorithms have been described here. Further articles on amplitude and derivative based QRS detection include [2], [4], [5], [6], [8], and [9].

2.3.3 Transform and Classification Based Algorithms

Signal transforms have also been used to detect peaks in the ECG.

Wavelet Based Algorithms:

The wavelet transform is used to obtain time and frequency characteristics of the signal and is closely related to the filter bank method [2]. The algorithm [19] for singularity detection and classification is utilized by most of the wavelet methods applied to ECG peak detection. QRS complex detection is achieved by using local maxima of the wavelet coefficients and the singularity degree which is the local Lipschitz requlrity, α, estimated from

$$\alpha_j = \ln\left|Wf\left(2^{j+1}, n^{j+1}\right)\right| - \ln\left|Wf\left(2^{j}, n^{j}\right)\right| \tag{2.14}$$

A review [7], provides application of wavelet analysis to the electrocardiogram.

Ability of Daubechies, spline and Morlet transforms to recognize and describe isolated cardiac beats are compared in [20].

[21],[22] used a first-order derivative of the Gaussian function as the wavelet in order to characterize ECG waveforms. They showed that the algorithm based on modulus maxima-based wavelet analysis with the dyadic wavelet transform performed well even in the signal corrupted modeled baseline drift and high frequency noise. They used this method in order to determine various waveforms and intervals such as the QRS complex width, T and P waves, and PR, ST and QT intervals. [23] described some improvements to this technique. [24] employed launch points and wavelet extreme in order to obtain amplitude and duration parameters from the ECG signal.

[25] utilized a method based on comparison of the modulus maxima with a threshold

obtained from preselected initial beats. The performance of the algorithm is improved by updating the threshold according to the recent signal and post precessing in order to remove redundant R waves or noise peaks. The performance of this algorithm when tested in MIT/BIH database is considered to be good with sensitivity and positive predictivity of 99.90% and 99.94% respectively. [26] is a extended version of this algorithm by means of including the premature ventricular contraction (PVC) beats. By employing a fuzzy neural network, [26] achieved a 99.79% accuracy in classification of PVC beats. [27] identified peaks, onsets and offsets of the QRS complexes, and P and T waves by using the algorithm of [25] applying a dyadic wavelet transform.

The algorithm implemented by [28], utilizes the local maximums of two consecutive dyadic wavelet scales and comparing them in order to identify the source of the local maximum as being due to either R wave or noise. Sensitivity and positive predictivity of this algorithm is reported to be 96.84% and 95.20% respectively when tested in American Heart Association (AHA) database.

[29] employed continuous wavelet transform (CWT) by extending the studies of [25] and [28]. Improved definition of the QRS modulus maxima curves are obtained by [29] because of the high time frequency resolution of their CWT based algorithm which allows better definition of spectral region corresponding to QRS maxima peak. Sensitivity and positive predictivity of this algorithm is 99.53% and 99.73% respectively when tested in Coronary Care Unit at the Royal Infirmary of Edinburgh database. Sensitivity and positive predictivity of this algorithm is 99.7% and 99.68% respectively when tested in MIT/BIH database.

Further articles on wavelet transform based QRS detection include [2], [4], and [7].

ANN Based Algorithms:

There are many neural network approaches on QRS detection proposed over the years such as multilayer perception (MLP), radial bases function (RBF), and learning vector quantization (LVQ) [4]. Figure 2.15 depicts the structure of MLP network. MLP

nerwork consist of several layers of interconnected neurons. In this network, each neuron represents a processing function:

$$y = f\left(w_0 + \sum_{i=1}^{N} w_i x_i \right) \tag{2.15}$$

where w_i is the weight assigned to input x_i. $f(.)$ can be a linear or a nonlinear function. If $f(.)$ is a nonlinear function, then in general it is defined as the logistic following function:

$$f(u) = \frac{1}{1+e^{-u}} \text{ or } f(u) = \tanh(u) \tag{2.16}$$

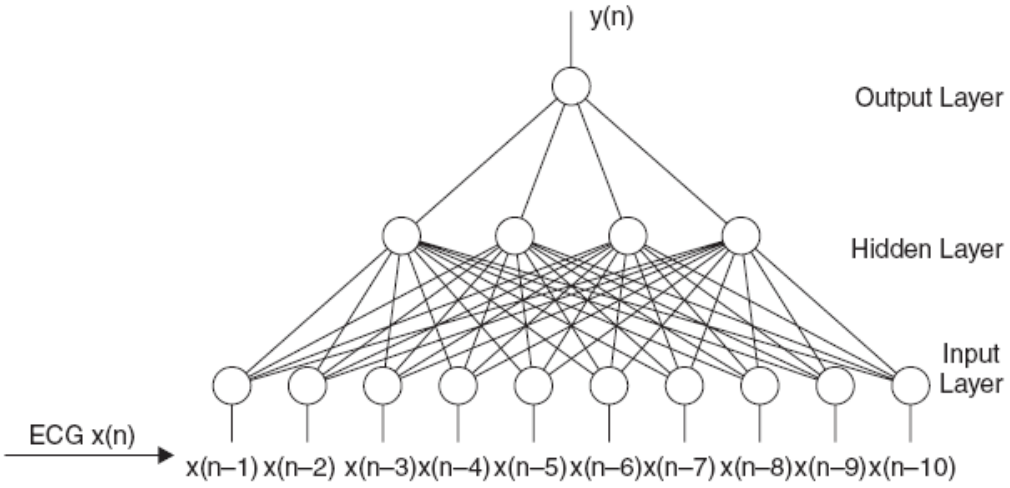

Figure 2.15 Multilayer perception [4]

RBF networks utilizes the following function:

$$y = \sum_{i=1}^{N} w_i \exp\left(-\frac{x(n) - c_i}{\sigma_i} \right) \tag{2.17}$$

where $x(n)$ is the input data vector, N is the number of neurons, w_i are the coefficients, c_i are the center vectors and σ_i are the standard deviations. Other

functions such as wavelets can be utilized instead of the exponential term in the equation.

An input layer, a competitive layer, and a linear layer constitute a LVQ network. Input vectors are automatically assigned to subclasses by the competitive layer where N is the maximum number of subclasses that equals to the number of competitive neurons. Competitive layer assigns the input vectors based on the Euclidian distance between the input vector and weight vector of each of the competitive neurons. Linear layer combines the subclasses in the competitive layer and the predefined target classes. Figure 2.16 depicts LVQ network structure.

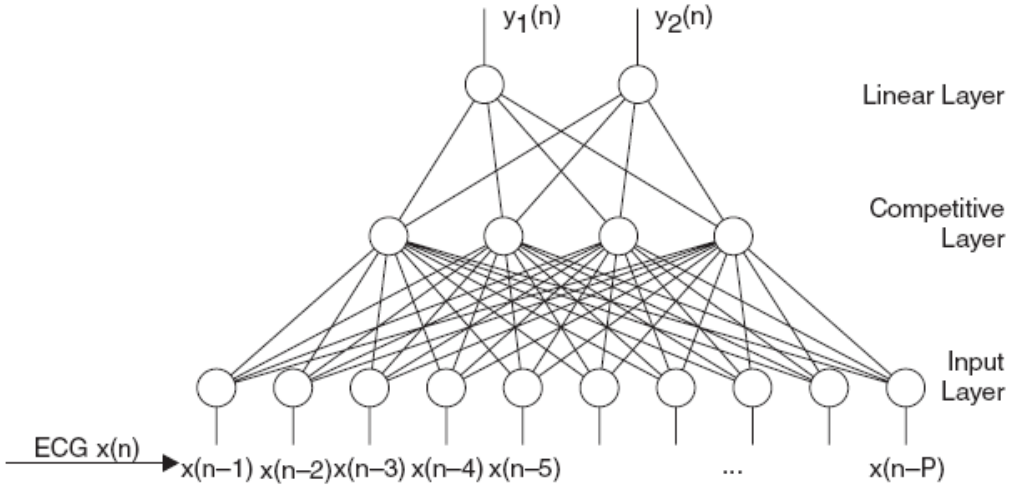

Figure 2.16 Structure of LVQ network [4]

Parameters of the networks must be trained prior to the QRS detection task. Training of MLP and RBF networks are accomplished by supervised learning algorithms and training of LVQ networks are accomplished by unsupervised learning algorithms

[31] has been developed an adaptive matched filtering algorithm based on multilayer perception neural network for QRS detection. The algorithm offers a sensitivity of 99.0 % and a positive predictivity of 98.5%.

[32] has been proposed a compression technique with back propagating neural

network algorithm in order to reduce the computational load and achieved 1.9% detection error rate (ER):

$$ER = \frac{FP + FN + U}{TB} \tag{2.18}$$

where FP is the number of false positives, FN is the number of false negatives, U is the unknown data and TB is the total number of QRS complexes.

[33] proposed a back propagating neural network algorithm with an average accuracy of 91.16%.

[30] employed ANNs as nonlinear predictors, in order to predict the value of the $x(n+1)$ from the previous samples. Then the network is trained to recognize the nonexistence of the QRS wave. The segments in which the portions of QRS wave exists, makes the output of the network to have large errors, $e(n)$, by which the QRS wave is detected. Since ECG signal contains more non-QRS segments than WRS segments, training the network to non-QRS segment prediction makes the network output convergent. QRS segments create sudden changes in the ECG signal lead sudden increase in the prediction errors, $e(n)$ which is utilized as the feature for QRS detection.

Further articles on neural network based QRS detection include [2] and [4].

Genetic Algorithms:

Genetic algorithms are used in designing optimal polynomial filters for ECG signals [34] for which quasilinear filters (with consecutive and selected samples) and quadratic filters (with selected samples) are applied. Since many possible combinations slows down the algorithm and exhaustive search is needed in order to achieve the best genes, genetic algorithms are not preferred much in ECG signal analysis.

Conclusion:

Major principles of software QRS detection has been described above. This field has matured to the extent where most of the algorithms available have been tried and tested on ECG recordings. In this thesis, four of the QRS detection algorithms that are known to be successful, are implemented and results are compared. A derivative based method (Method I) [6] and a digital filter based method (Method II) [6] which utilizes the fundamental concepts of QRS detection are implemented. Another method (Method III) [8] which utilized the morphological features which is known to be robust and popular by being the most cited reference is implemented. And a neural network based QRS detection method (Method IV) is implemented which is one of the promising technique as stated in the review chapter of [2].

2.4 Feature Extraction and Classification

Aim of feature extraction and classification is to identify and discriminate the important and special characteristics in ECG signal, associated with a particular pathology. Feature extraction is a very important issue in classification problem. Decision of which feature to extract or to select the features to be used in classification problem among extracted features is often implemented intuitively or heuristically by considering discrimination, reliability, independence, optimality of features as described below:

- **Discrimination:** The feature values of patterns in different classes should be as distinct as possible.
- **Reliability:** The feature values of patterns in the same class should be as close as possible.
- **Independence:** Correlation between features should be as small as possible.
- **Optimality:** Total number of features should be as small as possible.

Among to many feature extraction and classification methods in the literature, the common ones are highlighted in the following paragraphs emphasizing the importance of extracting and selecting the correct features in CVD classification.

One of the methods in ECG feature extraction is to utilize the morphological characteristics of the ECG. The morphological features such as maximum amplitude, RR duration, area under QRS waveform etc. can be extracted from detected QRS waves.

[35] compared the classification ability of the four classification methods (neural networks, K-th nearest neighbour rule, discriminant analysis and fuzzy logic) for normal beats and premature ventricular contractions by using morphological features. They achieved 82.1% specifity and 80.7% sensitivity by neural networks, 75.4% specifity and 80.9% sensitivity by K-th nearest neighbour rule, 88.5% specifity and 81.7% sensitivity by discriminant analysis, 82.8% specifity and 85.8% sensitivity by fuzzy logic.

[36] extracted twelve morphological features with Kth nearest neighbour classification rule, to classify five heart beat types (normal beats, left and right bundle branch blocks, premature ventricular contractions and paced beats) and achieved sufficiently high accuracies of 90.7% sensitivity and 95.5% specifity.

Another method in ECG feature extraction is to utilize the higher order statistics (HOS). Cumulants with orders higher than two and linear combinations of lower order cumulants are referred as HOS which are employed to minimize the spread of features belonging to similar type of heart rhythm [37], [38].

Another method in ECG feature extraction is to utilize wavelet transform [39]. Six energy descriptors to be employed as features can be derived from wavelet coefficients from a single beat interval. Additionally, nine different continuous and discrete wavelet transforms can be employed as features. Daubechies wavelet transform provides overall correct classification of 97,5% for ventricular fibrillation and ventricular tachycardia. [2].

One of the methods employed in heart beat classification is ANNs. Heart beat classification by ANN is first implemented by using MLP with back propagation algorithm [2]. [40] employed MLP for classification of normal and ventricular beats. [41] compared several ANN classifiers with accuracies 80% or above. [42] compared performances of MLP, LVQ and Kohenen's self organizing map in classification of normal and PVC beats and obtained better overall performance MLP network.

[43] proposed three ANN systems and in order to detect ventricular ectopic beats (VEB) by using AHA database. Two of the trained ANNs are used as local pattern recognizers for each record and the third one is used for global decision. This method improved the gross sensitivity from 94.83% to 97.39% and the gross positive predictivity from 92.70% to 93.58% with the ANN system in place.

Some of other classification algorithms developed using ANNs are such as [44], [45] and [46].

Conclusion:

Major principles of feature extraction and classification have been described above. Studies on extracting and selecting best features representing a unique disease type, which is not shared by the others is continuing with the goal of better classification.

In this thesis, morphological features are extracted, K-th nearest neighbor rule, artificial neural network, and a rule based classification algorithms are implemented, and results are compared.

2.5 Performance Evaluation

Sensitivity (Se) and positive predictivity (+P) are the essential parameters that are used to evaluate the performance of QRS detection algorithms [47]. A true positive (TP) is defined as a correctly detected or classified event, a false positive (FP) is defined as incorrectly detected or classified actually non-occurring event and a false negative (FN) is a missed event. Sensitivity is a measure of total detected beats

among all beats in the signal analyzed. Positive predictivity is a measure of true positive detected or classified beats among all detected or classified beats.

Related formulas are provided below:

$$Se = \frac{TP}{TP + FN} \tag{2.19}$$

$$+P = \frac{TP}{TP + FP} \tag{2.20}$$

In ideal case, both sensitivity and positive predictability are 1 or %100.

2.6 ECG Databases

There are several standard ECG databases available for performance evaluation of detection and classification of algorithms such as MIT-BIH Database, AHA Database, Ann Arbor Electrogram Libraries, CSE Database, European ST-T Database, QT Database, MGH Database, IMROVE Data Library, ECG Reference Data Set.

MIT-BIH Database is a well-annotated and validated database of real ECG records that is provided by MIT and Boston's Beth Israel Hospital. For QRS occurrence annotations, a slope-sensitive QRS detector is used, then the results were evaluated by two cardiologists working independently. Then, their annotations are compared and agreement is done between the results. However, a few unclassified beats are remained due to disagreement between the two cardiologists [48].

MIT-BIH Database contains various databases for various conditions such as Arrhythmia Database, Noise Stress Test Database, Ventricular Tachyarrhythmia Database, ST Change Database, Malignant Ventricular Arrhythmia Database, Atrial Fibrillation/Flutter Database, ECG Compression Test Database, Supraventricular Arrhythmia Database, Long-Term Database, and Normal Sinus Rhythm Database. Furthermore, the records are corrupted by noise and artifacts which makes QRS detection and heatbeat classification challenging [2].

Among these several standard databases of MIT-BIH, Arrhythmia Database is the most frequently used one for the performance evaluation of the QRS detection and arrhythmia classification algorithms. In addition, this database includes various Holter type ECG recordings of two leads that are rarely observed but clinically important. One of the lead is usually MDII (Modified Lead II) and the other one is either one of the Lead 1 (V1), Lead 2 (V2), Lead 3 (V3), Lead 4 (V4), Lead 5 (V5), Lead 6 (V6).

A record from MIT-BIH Arrhythmia Database with annotations are provided in Figure 2.17 [49].

Figure 2.17 A recording from MIT-BIH database (MITDB 233 record [49])

CHAPTER 3

METHODS

This chapter starts with the explanation of the prefiltering stage, followed with the details of the QRS detection, the feature selection and the classification algorithms implemented in this thesis.

3.1 Prefiltering

The first stage in QRS detection is the prefiltering stage. In this stage, the raw ECG signal is filtered in order to suppress the noise, and enhance the characteristic features of QRS complex, as explained in detail in section 2.2. One can utilize infinite impulse response (IIR) or finite impulse response (FIR) filters for this prefiltering stage.

Infinite impulse response (IIR) filters are recursive filters that have the advantage of less computation than the finite impulse response (FIR) filters. However, nonlinear phase response of IIR filters causes phase distortion. Applying the IIR filter to the ECG signal in both directions is referred as the "zero phase IIR filter" and it is a solution to phase distortion problem in a way that distortions occurred by filtering the signal in one direction is corrected by filtering the signal in the reverse direction [3].

For prefiltering, a band pass filter composed of cascaded bidirectional high pass filter and bidirectional low pass filter is obtained. Butterworth filter, which is a special kind of an IIR filter, has the advantage of having no ripples in either the pass band or the stop band, and thus implemented in this study for both the high pass and the low pass filtering stages. The resultant band pass filter has no ripples in either the pass band or the stop band and zero phase with cut of frequencies 0.67 Hz and 35 Hz. In the literature in general, band pass filters covering 10 Hz to 25 Hz are used for QRS detection [4]. Although these filters extract the characteristic features of QRS complex, some distortions in the wave shape of the ECG signal are usually

encountered since ECG signal energy is accumulated on a frequency band covering up to 40 Hz [5]. In this study, cut off frequencies are chosen such that the noise is attenuated while not distorting the ECG signal itself. Lower cut off frequency of 0.67 is chosen because the slowest heart rate which is thought to be 40 bpm implies the lower cut off frequency to be greater that 0.67 Hz [3]. Higher cut off frequency of 35 Hz, which is found empirically, is chosen because it is the lowest frequency covering the QRS complex while keeping the ECG signal undistorted.

Figure 3.1 depicts the algorithm of the bidirectional filtering where x[n] is the raw ECG data, h[n] is the fifth order Butterworth IIR filter and "flip" step depicts the time reversal of the signal. This algorithm starts with applying the fifth order high pass Butterworth IIR filter having a cut-off frequency of 0.67 Hz to x[n]. This resultant signal is then flipped and passed through the same filter again. Finally, the resultant signal is flipped one more time. The frequency response of the fifth order high pass Butterworth IIR filter is depicted in Figure 3.2.

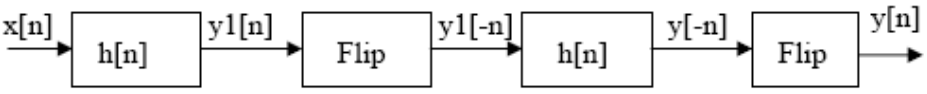

Figure 3.1 Block diagram of a bidirectional filter.

After this high pass filtering stage, the same procedure is applied to the output of the high pass filtering stage with a fifth order low pass Butterworth IIR filter having a cut-off frequency of 35 Hz. The frequency response of the fifth order low pass Butterworth IIR filter is depicted in Figure 3.2.

An example of ECG data before filtering and after filtering are depicted in Figure 3.4.

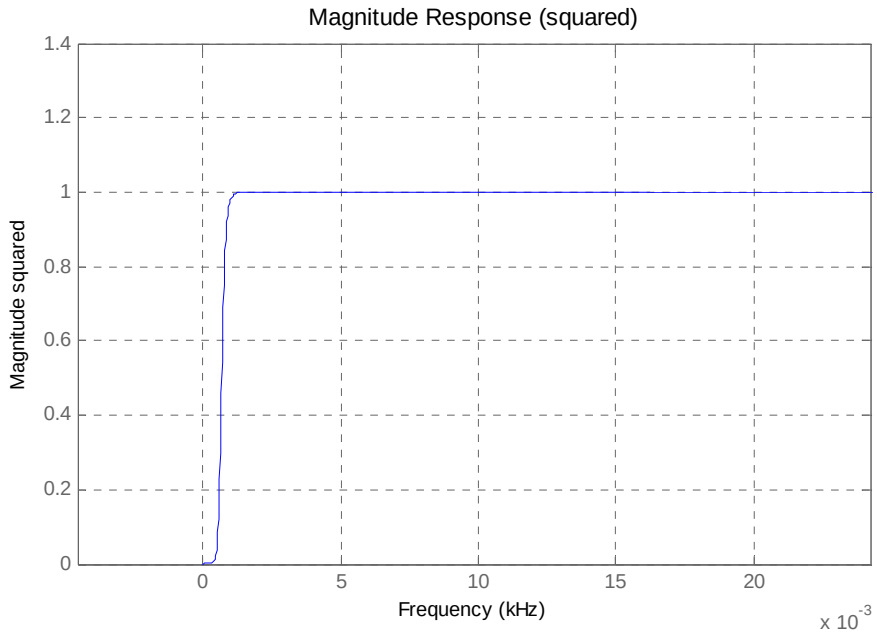

Figure 3.2 The frequency response of the Butterworth IIR high pass filter

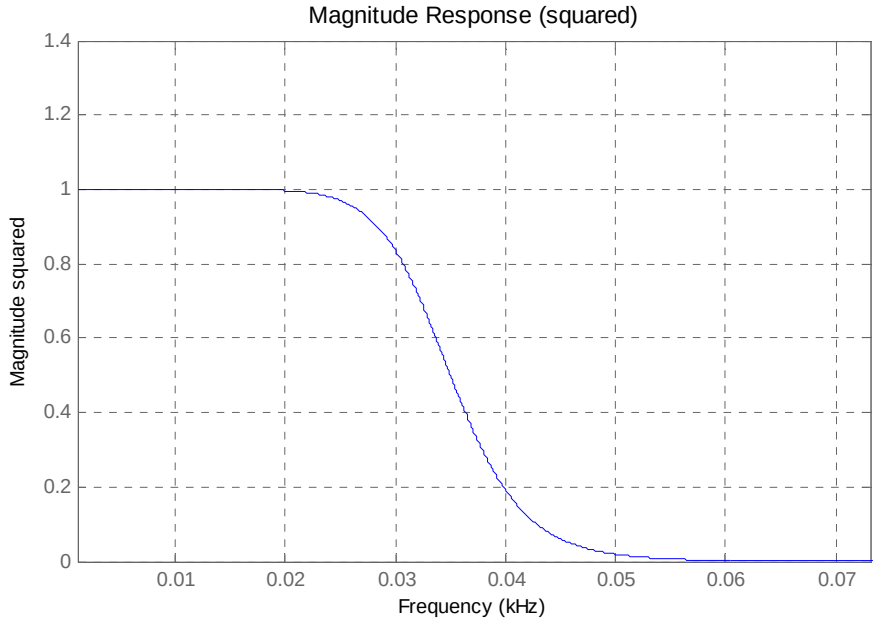

Figure 3.3 The frequency response of the Butterworth IIR low pass filter

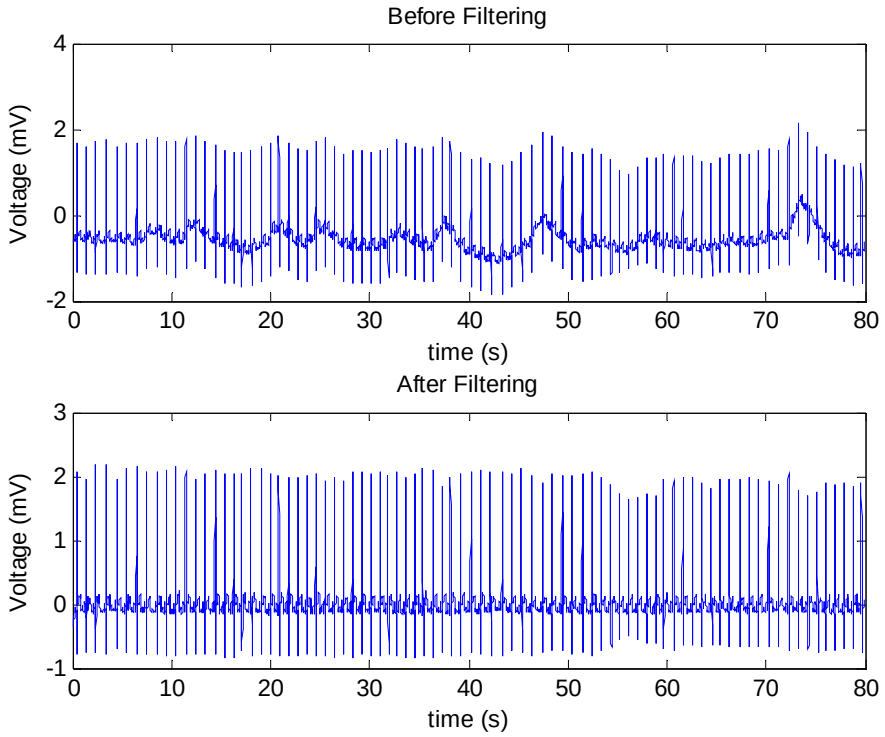

Figure 3.4 An example illustrating the effect of filtering on ECG data

3.2 QRS Complex Detection

In this thesis, four of the QRS detection algorithms from literature that have been known to be successful are implemented and their results are compared. These methods are:

- (Method I) A derivative based method [6],
- (Method II) A digital filter based method that utilizes the fundamental concepts of QRS detection [6],
- (Method III) Tompkin's method [8], that utilizes the morphological features of the ECG signal. This method is known to be robust and and popular by being the most cited reference,

- (Method IV) A neural network based QRS detection method, which is one of the most promising techniques as stated in the review chapter of [2].

The algorithms in this study are not the exact copy of the algorithms in literature, and they should be considered as adaptations of the generic concepts.

3.2.1 QRS Complex Detection – Method I

QRS complex has not always the highest amplitude in a cardiac cycle due to artifacts, but it has the highest slope in a cardiac cycle. Therefore, differentiation forms the basis of many QRS detection algorithms. Differentiation is a way of realization of a high pass filter by amplifying the higher frequency components (QRS complex) and attenuating the lower frequency components (P and T waves) in an ECG signal.

QRS detection algorithm implemented by [6] forms the basis of the differentiation algorithm implemented in this thesis. In this method, a variable derived from a weighted summation of first and second derivatives of the ECG signal is scanned and if certain duration within a window exceeds the threshold, this segment is taken as part of the QRS complex. Then the point having the maximum first derivative with in the group is taken as the QRS complex. Signal processing steps of this algorithm are given below.

1. "$x(nT)$" is defined as the ECG signal as depicted in Figure 3.5.

2. Absolute values of the first and second derivatives of the ECG signal are calculated as depicted in Figure 3.6 and Figure 3.7.

$$y0(nT) = |x(nT) - x(nT - 2T)|, \text{ first derivative} \quad (2.1)$$

$$y1(nT) = |x(nT) - 2 * x(nT - 2) + x(nT - 4)|, \text{ second derivative} \quad (2.2)$$

3. The first and second derivatives ($y0(nT)$ and $y1(nT)$), are scaled and then summed as depicted in Figure 3.8.

$$y2(nT) = 1.3 * y0(nT) + 1.1 * y1(nT) \quad (2.3)$$

4. The points at which the scaled sum of the first and second derivatives ($y2(nT)$) exceeds a certain threshold is found.

   $z(nT) = 1$ If $y2(nT) \geq (\alpha / 50) * (1000 / samplingrate)$

   $z(n) = 0$, otherwise (2.4)

   where α is the local maximum of $y2(nT)$ around the point of interest.

5. Then over-threshold values are scanned and whenever an over-threshold value is detected, the next time interval of 440 ms are scanned. If 300 ms within this 440 ms window exceed the threshold, this segment is taken as part of a QRS complex. The first sample at which the threshold is exceeded is taken as the point of detected QRS complex.

A tuning procedure is applied to parameters in threshold stages until the best results are obtained.

In some diseases such as left bundle branch block, two R waves may appear within one QRS complex, which causes the algorithm to detect false positives. We have added an extra step to improve the performance of the algorithm. This step includes not looking for another QRS complex for a duration of 0.1 seconds, which is the maximum possible QRS duration, whenever a QRS complex is detected.

Besides detecting the QRS complex, this algorithm (the output of the scaled sum of the first and second derivatives) can also be used to extract a feature proportional to the duration of the QRS complex.

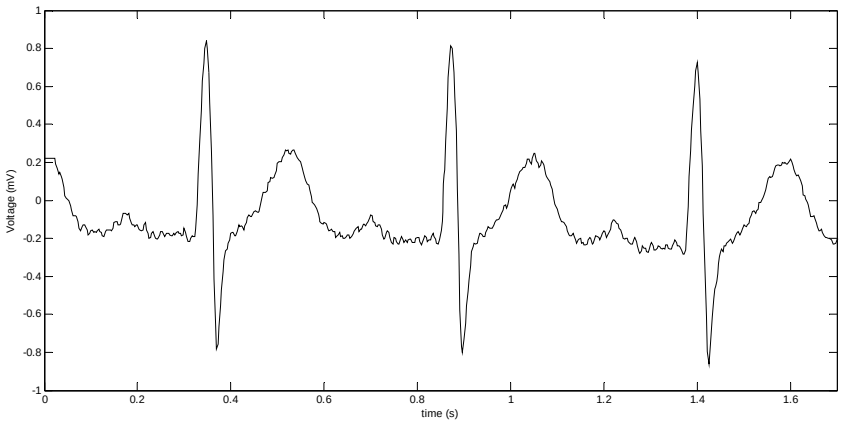

Figure 3.5 x(t), An example of the ECG signal

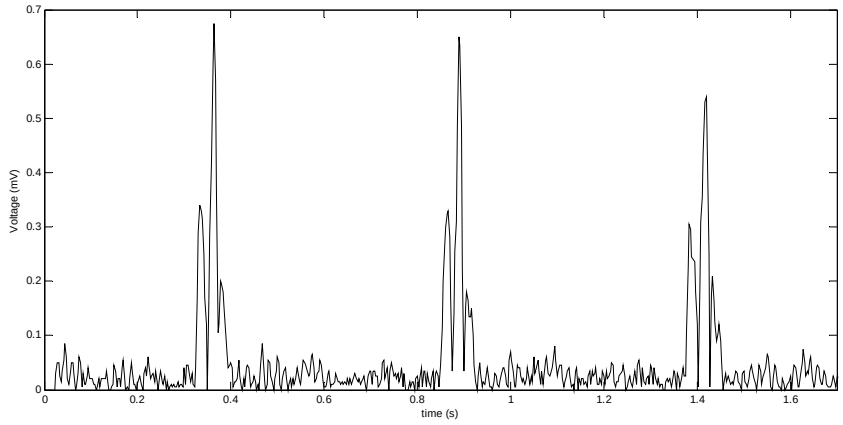

Figure 3.6 y0(t), Rectified first derivative

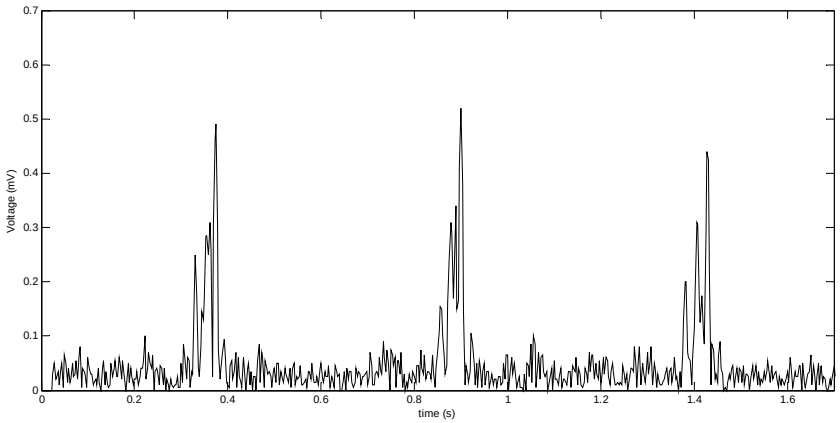

Figure 3.7 y1(t), Rectified second derivative

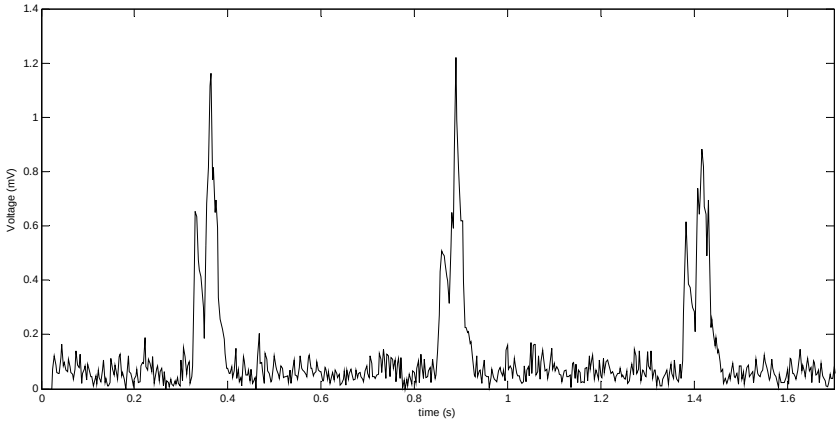

Figure 3.8 y2(t), Scaled sum of rectified 1st and 2nd derivatives

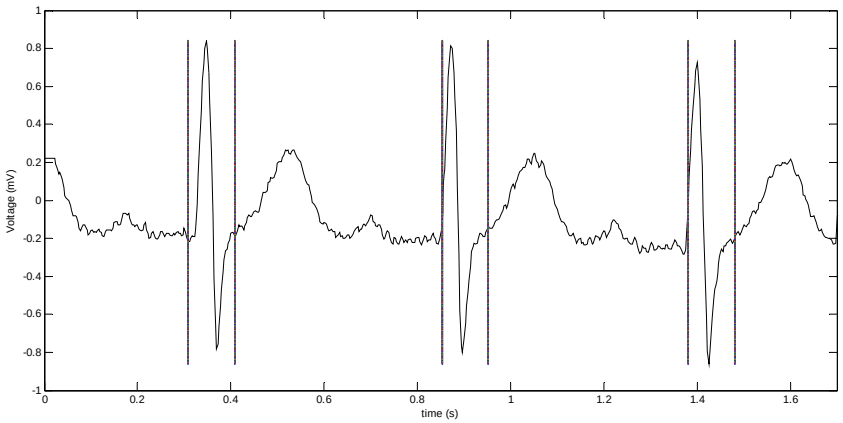

Figure 3.9 Detected QRS complexes with starting and ending instants indicated (vertical lines)

3.2.2 QRS Complex Detection – Method II

QRS detection algorithm implemented by [6] forms the basis of the digital filter algorithm implemented in this thesis. In digital filter QRS detection method, waveforms in ECG signal other than the QRS complex are removed by using a band pass filter. This filtering is applied in two steps: First the signal is low pass filtered in order to eliminate unwanted high frequency components by using a three point moving average filter, then put through a stricter low pass filter by using a 28 ms moving average filter. Next, the output of the second low pass filter is subtracted from the output of the first one in order to obtain the band pass filtered signal. This result is then squared in order to make all differences positive and enhances the high frequency content of the QRS complex. Since QRS complex contains the higher frequency band of the remaining components of the signal, multiplying the result of the previous step by 28 ms moving average filter further enhances QRS complex and suppress small values with the cost of smoothing the peak of the QRS complex. Q, R and S points are relatively symmetrical shaped whereas baseline drift is usually not symmetrical. In order to distinguish between QRS complex and spurious peaks due to baseline drift, the peaks with no symmetry in the time axis for duration of 28 ms are eliminated. Finally, the points below a threshold are set to zero, and the over-

threshold points within a 144 ms interval are grouped together. Flow chart of this algorithm is depicted in Figure 3.10 and signal processing steps are given below:

1. "$x(nT)$" is defined as the ECG signal as depicted in Figure 3.11:

2. "$x(nT)$" is smoothed using a three-point moving average filter as depicted in Figure 3.12:

$$y0(nT) = \frac{[x(nT - T) + 2 * x(nT) + x(nT + T)]}{4} \quad \text{for } n = 2 : lenght(x) - 1 \tag{2.5}$$

3. Output of the moving average filter is passed through a low pass filter as depicted in Figure 3.13:

$$y1(nT) = \left[\frac{1}{2m+1}\right] \sum_{k=n-m}^{n+m} y0(kT) \quad \text{for} \quad n = m + 1 : lenght(y0) - m, \quad \text{where m}$$

corresponds to a 12 ms duration ($m = 3$ for 250 sps) (2.6)

4. Difference between the expression in (2.6) and (2.7) is squared as depicted in Figure 3.14:

$$y2(nT) = [y0(nT) - y1(nT)]^2 \quad \text{for } n = 1 : lenght(y1) \tag{2.7}$$

5. Squared difference of (2.8) is filtered as depicted in Figure 3.15:

$$y3(nT) = y2(nT) \left[\sum_{k=n-m}^{n+m} y2(kT)\right]^2 \quad \text{for} \quad n = m + 1 : lenght(y2) - m, \quad \text{where where m}$$

corresponds to a 12 ms duration ($m = 3$ for 250 sps) (2.8)

6. The following array is formed for $n = m + 1 : length(y3)$ as depicted in Figure 3.16:

$$y4(nT) = y3(nT), \text{ if } [(y0(nT) - y0(nT - mT)) * (y0(nT) - y0(nT + mT))] > 0$$

$$y4(nT) = 0, \text{ otherwise} \tag{2.9}$$

7. Over threshold samples of $y4(nT)$ are scanned according to the following threshold definition:

$$threshold = 0.01 * \max(y4(nT : nT + samplingrate * 2))$$

$$\text{for } n = 1 : length(y4(nT)) - samplingrate * 2 \tag{2.10}$$

8. Local maximum around over threshold samples is considered as a part of QRS complex as depicted in Figure 3.17.

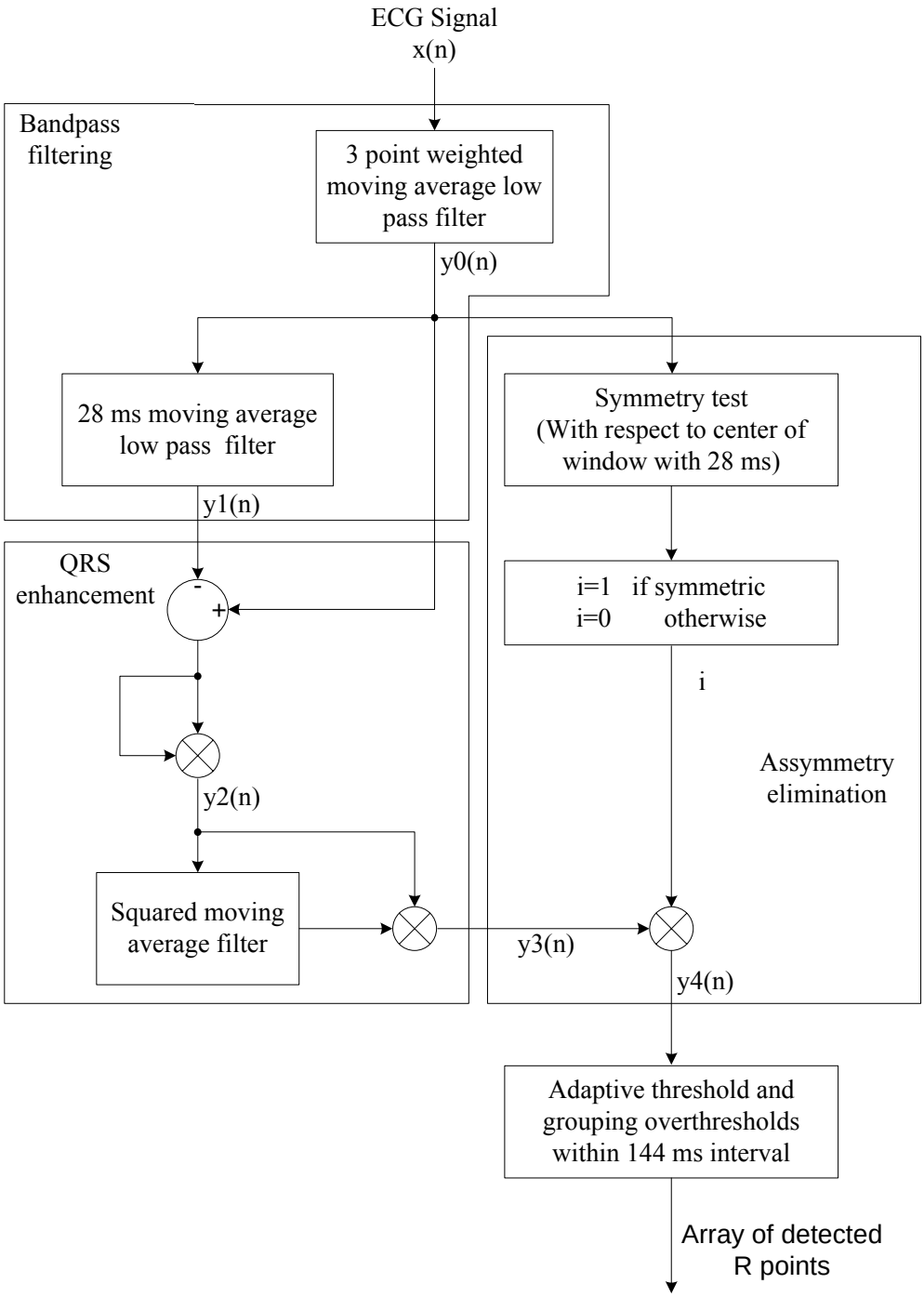

Figure 3.10 Flowchart of digital filter based QRS detection algorithm.

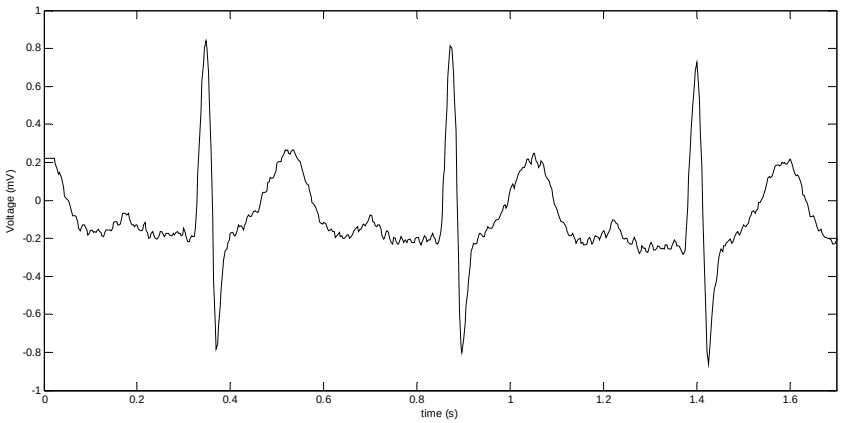

Figure 3.11 x(t), An example of input ECG signal

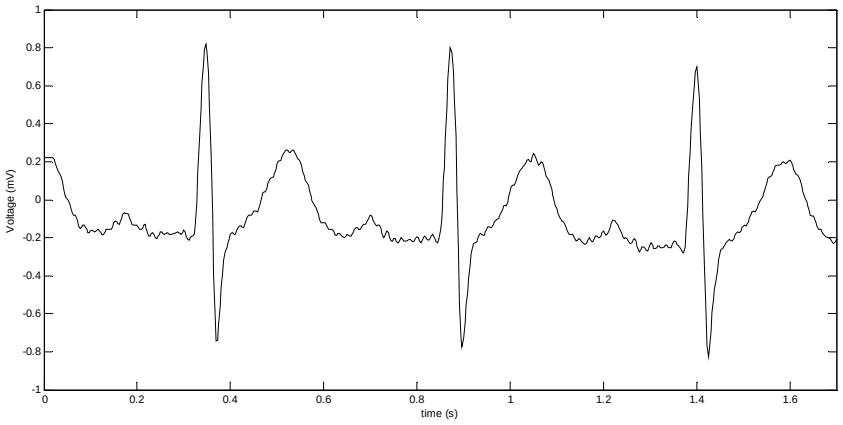

Figure 3.12 y0(t) after moving average filtering.

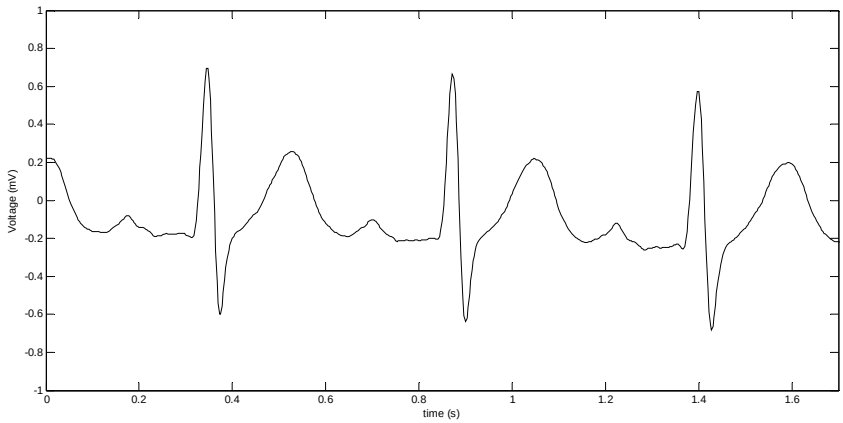

Figure 3.13 y1(t) after low pass filtering.

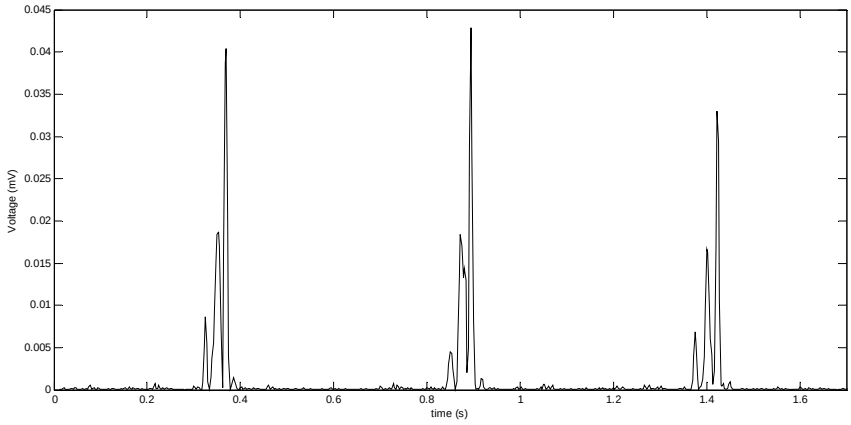

Figure 3.14 y2(t) after square of the low pass filter input and output difference.

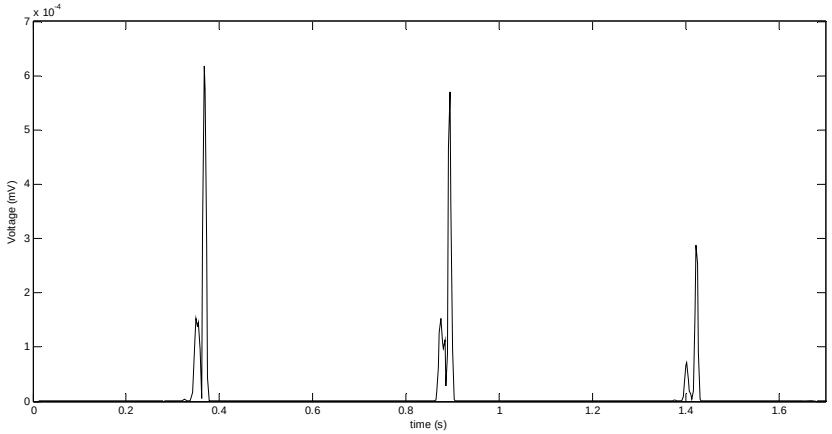

Figure 3.15 y3(t) after filtering of squared difference.

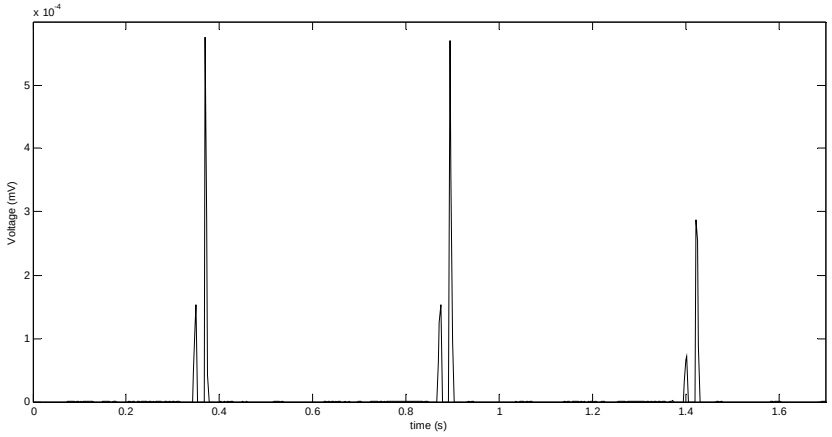

Figure 3.16 y4(t) array after logical operation.

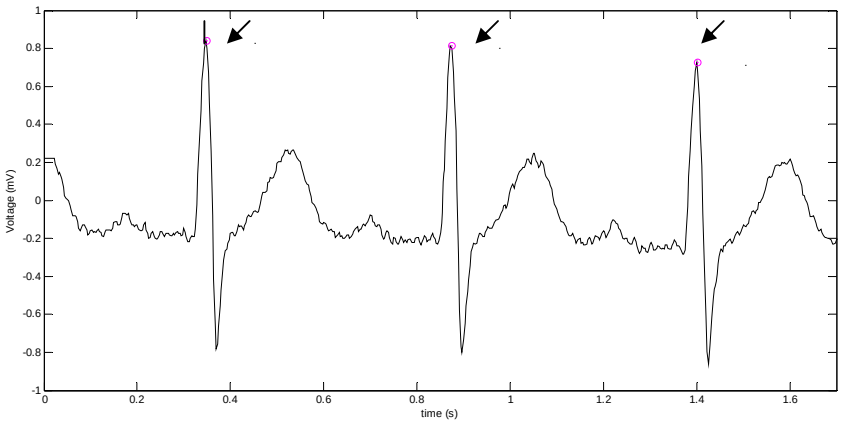

Figure 3.17 Detected QRS complexes

3.2.3 QRS Complex Detection – Method III

Algorithm implemented by [8], forms the basis of this QRS algorithm implemented in this thesis. This algorithm employs slope, amplitude and width features of the QRS complex for detection. The processing steps of this algorithm are depicted in Figure 3.18. The ECG signal is first passed through a band pass filter formed by cascading a low pass filter and a high pass filter in order to attenuate the noise. Then differentiation, squaring, and time averaging processes are applied to the signal.

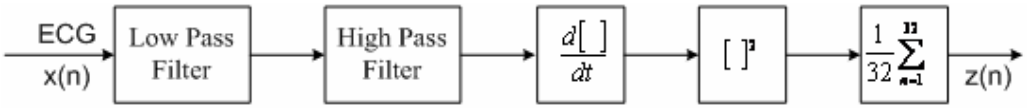

Figure 3.18 Processing steps for QRS detection with Method III.

Band pass filter enhances the frequency band around 10 Hz at which the signal to noise ratio of QRS complex is at its maximum. The lower frequency band attenuated by the band pass filter includes the P wave, the T wave and the baseline drift. The higher frequency band attenuated by the band pass filter includes the electromyographic noise and the power line interference.

Differentiation, which is a nonlinear process, is the next step. Differentiation is employed in order to extract the high slopes. This step distinguishes the QRS complex from the other components that constitute an ECG signal.

Then a nonlinear transformation is applied to the signal during which the signal samples are squared point by point. This transformation is applied in order to make the entire signal samples positive before the next integration step and enhance the higher frequencies of the signal, which are normally constituted by QRS complexes mostly.

Then a moving window integrator is applied to the signal at which the area under the squared waveform over a 150-ms interval is summed. After summation of a 150-ms interval, one sample is advanced and the following 150-ms interval is summed for the next sample. The width of the interval is chosen to be 150 ms. so that time duration of extended abnormal QRS complexes are covered while overlapping of QRS complexes and following T waves are prevented.

Adaptive amplitude thresholds are applied to the resultant signal in order to determine the occurrence of the QRS wave.

Each of the stages in this QRS detection method are explained in detail in the following sections. Figure 3.19 depicts an example of input ECG signal.

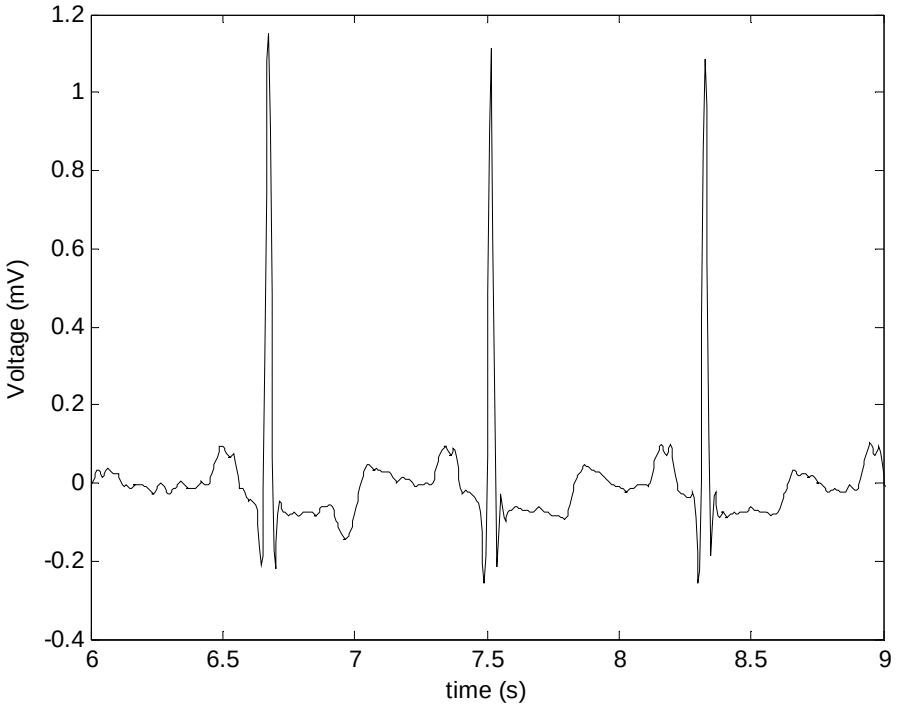

Figure 3.19 An example of input ECG signal

3.2.3.1 Band Pass Integer Filter

The band pass filter attenuates the noise in the ECG signal by covering only the spectrum of QRS complexes. Therefore, it suppresses the EMG artifacts, power line interference, baseline drift, and T-wave interference. QRS energy is cumulated approximately in the 5-15 Hz range and the band pass filter enhances this band while attenuating the rest. The band pass filter, which is constituted by cascaded low pass and high pass filters, is a recursive integer filter at which zeros are canceled by the poles on the unit circle of the z-plane.

Low Pass Integer Filter:

The second-order low-pass filter is implemented with the following transfer function:

$$H(z)=\frac{\left(1-z^{-6}\right)^2}{\left(1-z^{-1}\right)^2} \tag{2.11}$$

The difference equation of the filter is:

$$y(n)=2y(n-1)-y(n-2)+x(n)-2x(n-6)+x(n-12) \tag{2.12}$$

The filter has a cut off frequency around 11 Hz with 5 samples (corresponding to 25 ms for a sampling rate of 200 sps) delay, and gain of 36.

Magnitude and phase responses of the low pass filter are depicted in Figure 3.20. The phase response of the filter is purely linear. Power line interference is attenuated by more than 35-dB attenuation of the frequency corresponding to 0.3 f/fs, which is 60 Hz for sampling rate of 200 sps.

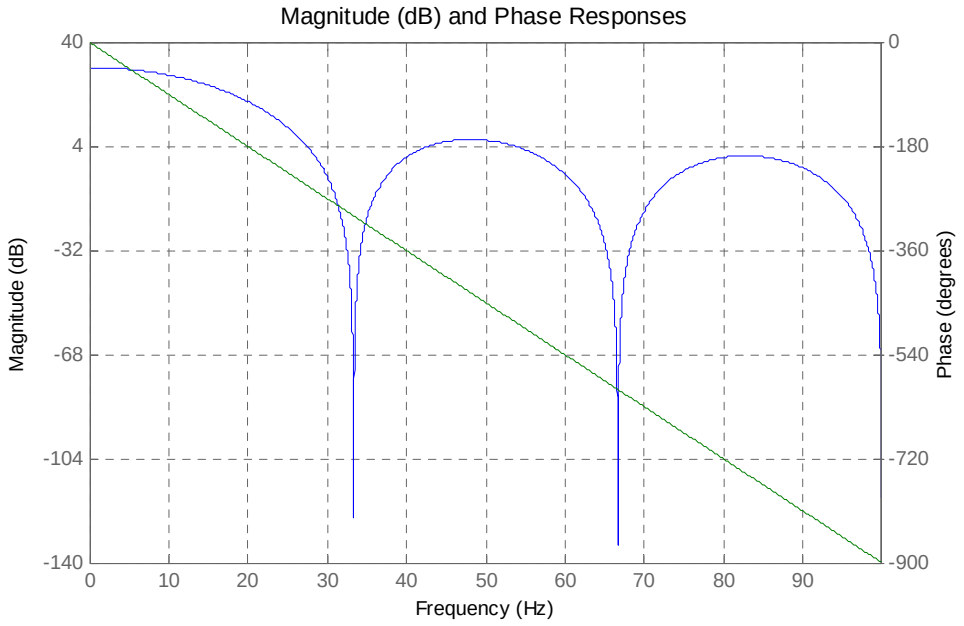

Figure 3.20 Low pass filter amplitude and phase responses

High Pass Integer Filter:

Figure 3.21 depicts the high-pass filter, which is constituted by subtracting a first order low-pass filter from an all-pass filter with some delay.

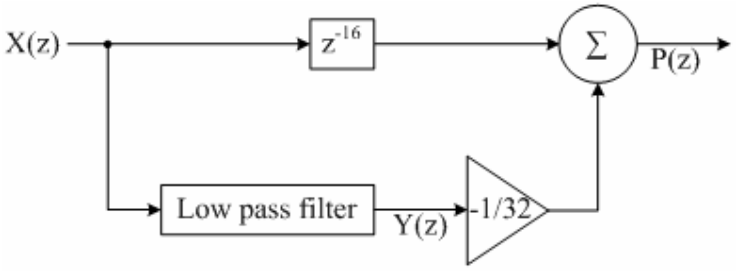

Figure 3.21 The high pass filter is implementation

The integer coefficient low pass filter is implemented by the following transfer function:

$$H_{lp}(z)=\frac{Y(z)}{X(z)}=\frac{1-z^{-32}}{1-z^{-1}} \tag{2.13}$$

The difference equation of the low pass filter is:

$$y(nT)=y(nT-T)+x(nT)-x(nT-32T) \tag{2.14}$$

This low pass filter has a dc gain of 32 and a delay of 15.5 samples. The low pass filter is divided by its dc gain 32, then the resultant signal is subtracted from the original signal with delay in order to constitute the high pass filter. The high pass filter has the following transfer function:

$$H_{hp}(z)=\frac{P(z)}{X(z)}=z^{-16}-\frac{H_{lp}(z)}{32} \tag{2.15}$$

The difference equation of this filter is:

$$p(nT)=x(nT-16T)-\frac{1}{32}\left[y(nT-T)+x(nT)-x(nT-32T)\right] \tag{2.16}$$

This filter has its lower cut-off frequency at around 5 Hz, a delay of 16T (corresponding to 80 ms), and 1 as the gain. Figure 3.22 depicts the magnitude and phase response of the high pass filter, which has a purely linear phase.

The resultant signal after the ECG signal depicted in Figure 3.19 is passed through the band pass filter is shown in Figure 3.23.

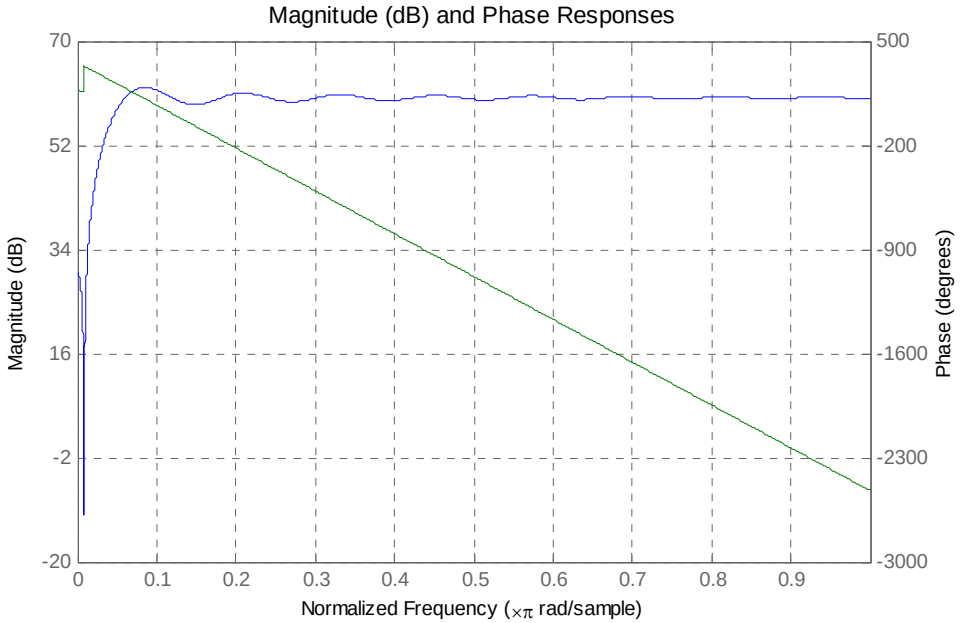

Figure 3.22 Magnitude and phase responses of the high pass filter

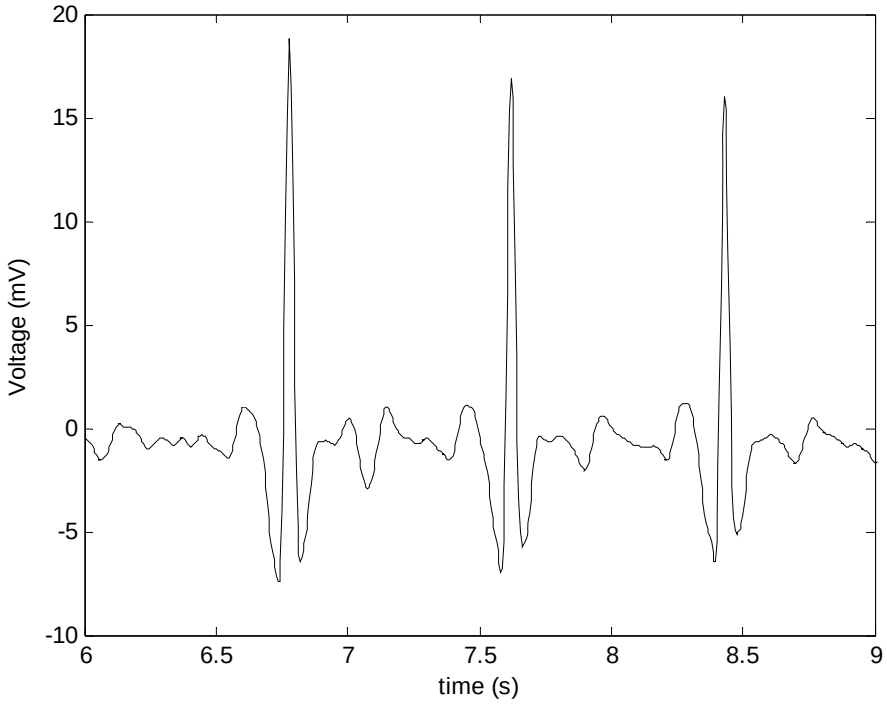

Figure 3.23 Band pass filtered ECG signal

3.2.3.2 Derivative

After the filtering process, the ECG signal is passed through the differentiation step in order to extract the high slope characteristic of the QRS complex. A five point derivative with the following transfer function is employed:

$$H(z) = 0.125\left(2 + z^{-1} - z^{-3} - 2z^{-4}\right) \tag{2.17}$$

The corresponding difference equation with a delay of 2T (correspond to 10 ms):

$$y(nT) = \frac{2x(nT) + x(nT - T) - x(nT - 3T) - 2x(nT - 4T)}{8} \tag{2.18}$$

Figure 2.24 depicts the resultant ECG signal after band pass filtering and differentiation operations. In this figure, attenuation of P and T waves and

enhancement in peak to peak QRS complex can be seen.

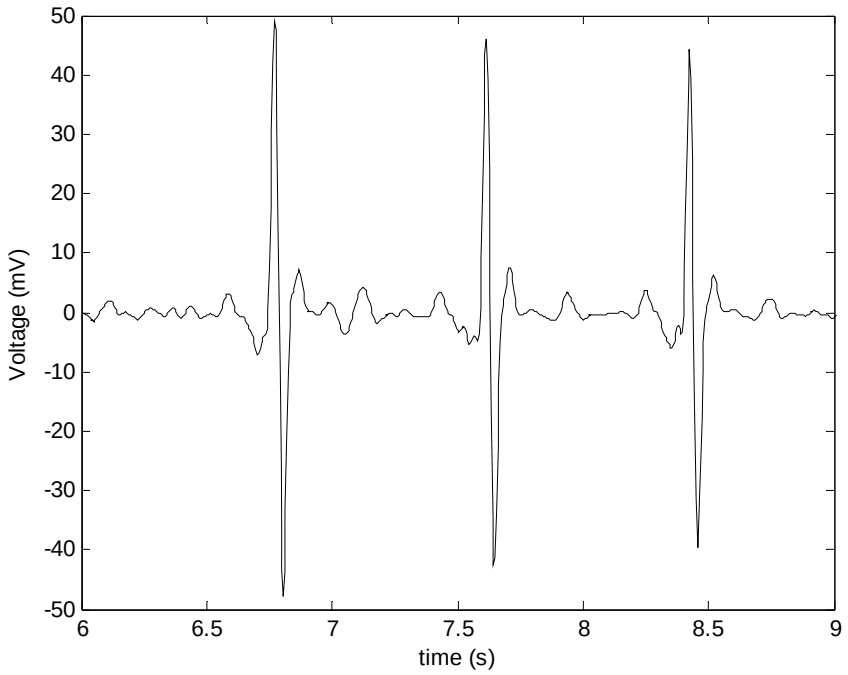

Figure 3.24 ECG signal after band pass filtering and derivative operations

3.2.3.3 Squaring Function

The squaring function, which is a nonlinear process, is implemented with the following equation:

$$y(nT) = [x(nT)]^2 \tag{2.19}$$

All samples in the ECG signal become positive after this operation, which is important prior to the following integration process. This operation also nonlinearly amplifies the output of the previous derivative operation, which contained enhanced QRS complexes and suppressed non-QRS components.

Figure 3.25 depicts the resultant signal after band pass, differentiation and squaring operations.

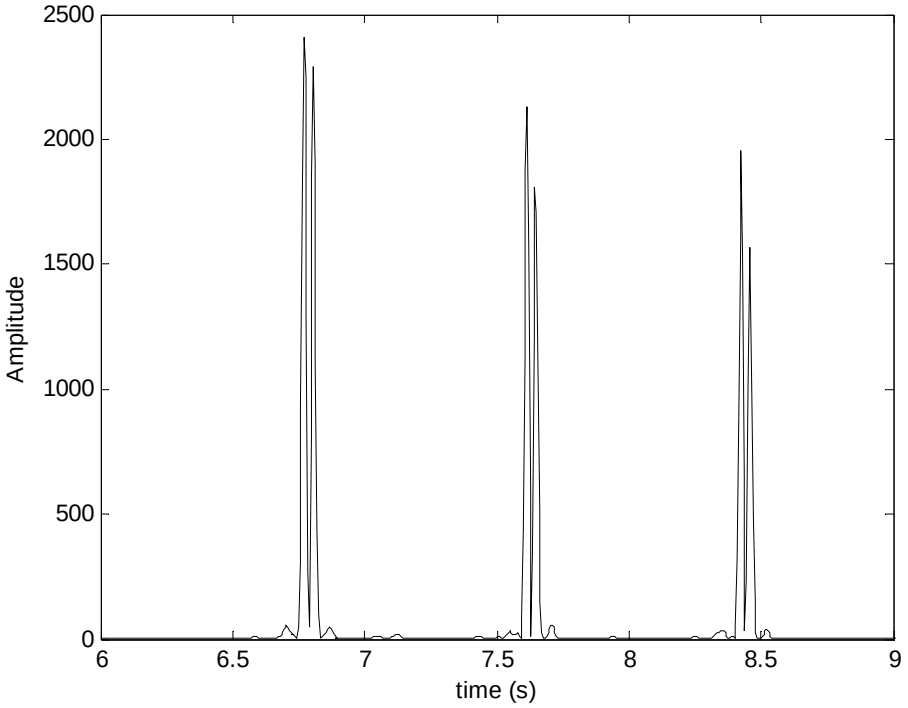

Figure 3.25 The signal after squaring operation

3.2.3.4 Moving Window Integral

The slope information not always characterizes a QRS complex, because there are many pathologic QRS complexes with large amplitudes and long durations but not steep slopes. Therefore, moving window integration is employed in order to extract further information from the signal for QRS detection.

Moving window integration is implemented with the following difference equation:

$$y(nT) = \frac{1}{N}\left[x(nT - (N-1)T) + x(nT - (N-2)T) + ... + x(nT)\right] \tag{2.20}$$

where N is the number of samples in the moving window corresponding to the width of the window. The value of N is chosen in order to optimize the following considerations:

- N should be great enough so that the window covers the widest possible QRS complex.

- N should be small enough so that the window does not cover QRS complex and the T following T wave at the same time.

Therefore, the width of the window is chosen to be 150 ms corresponding to 30 samples for a signal with sampling rate of 200 sps.

Figure 3.26 depicts the resultant signal after band pass filtering, differentiation, squaring and moving window integration operations.

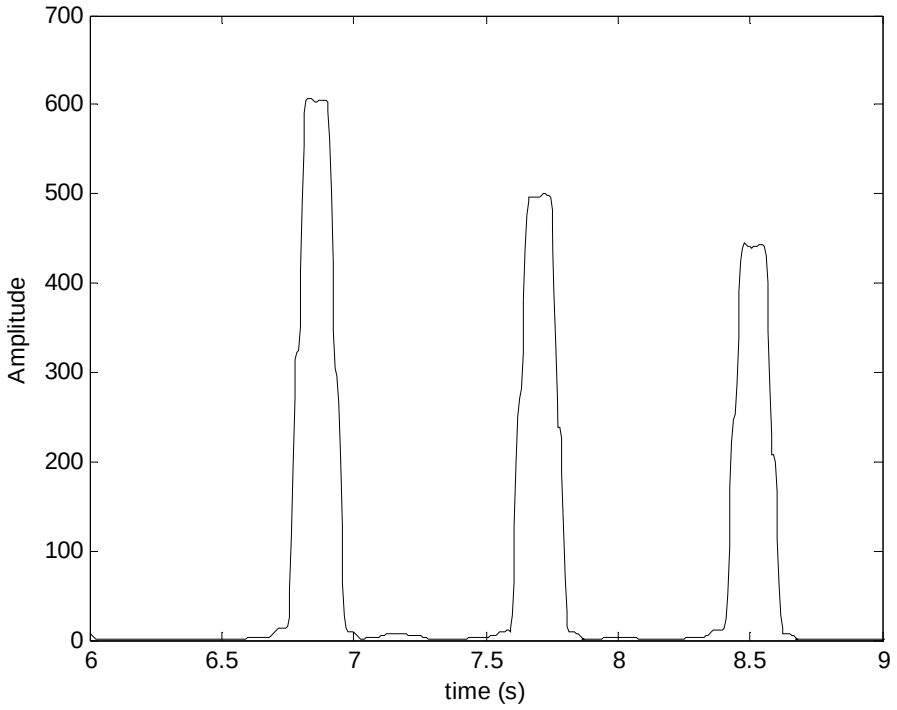

Figure 3.26 Signal after moving window integration

3.2.3.5 Thresholding

Output of the moving window integration is scanned for points exceeding local threshold given below:

$$threshold = \frac{\max\left(y5\left(n : n + samplingrate * 2\right)\right)}{11} \tag{2.21}$$

Then, over-threshold values are scanned and whenever an over threshold value is detected the next time interval of 6 ms is scanned and if 4.6 ms within this 6 ms window exceed the threshold, this segment is taken as part of a QRS complex. The maximum first derivative within this segment is taken as the point of the detected QRS complex. The detected QRS complexes are depicted in Figure 3.27.

The same step as described in section 3.2.1, regarding not looking for another QRS complex for a duration of 0.1 seconds is applied to this method. In addition, a tuning procedure is applied to parameters in threshold stages until the best results are obtained.

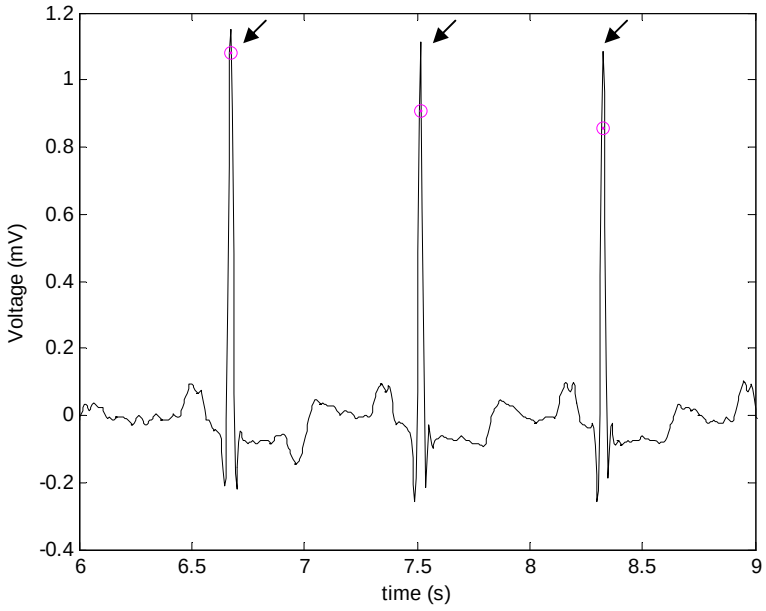

Figure 3.27 Detected QRS complexes

3.2.4 QRS Complex Detection – Method IV

MLP based QRS detection algorithm described by [4] forms the basis of the this algorithm implemented in this thesis. In this algorithm, QRS complexes are recognized by a multilayer perceptron (MLP) which is a feed-forward artificial neural network model that maps sets of input data onto a set of appropriate output model [50]. In this study, two layers of neurons (nodes) are used with nonlinear activation functions which can distinguish ECG data that is not linearly separable or separable by a hyperplane [51]. A nonlinear activation function which is normalizable and differentiable is used for each neuron in the MLP. A sigmoid activation function is used that is described by $f(u) = \frac{1}{1+e^{-u}}$ with a range of 0 to 1. The network consists of an input and an output layer with one hidden layer in between. The number of neurons in the input and the hidden layers are determined experimentally until the best results are obtained. Thus, network is constructed such that there are 21 nodes in the input layer, 5 neurons in the hidden layer and 1 neuron at the output layer.

The ECG signals are down sampled to 100 sps which covers the frequency band of ECG signals in order to decrease the computational load and increase the computational speed.

The input data set which is fed into the network for both training and test purposes, consists of a set of input vectors that correspond to the values of the ECG in a 200 ms sliding window as depicted in Figure 3.28. The number of variables of an input vector is 21 samples (1 sample for the positive peak, 10 samples for the prior of the positive peak and 10 samples after the positive peak).

In order to define the weights of the network, a set of training vectors are fed into the input layer of the network with the target output defined as either 0.999 when the QRS is centered in the window or 0.001 otherwise. Figure 3.29 depicts an example of target outputs for vectors of the input signal depicted in Figure 3.28.

After then test vectors are is fed into the network sequentially, and a threshold stage is

applied to the signal at the output node in order to locate the QRS complexes. This actual signal obtained at the output node is not the same as the target output defined above as expected. However, it has such a form that the QRS regions have peaks, which is detectable by a simple threshold stage.

Figure 3.30 depicts the actual signal obtained from the output node, when sliding windows from the input signal depicted in Figure 3.28 is fed in to the input layer sequentially.

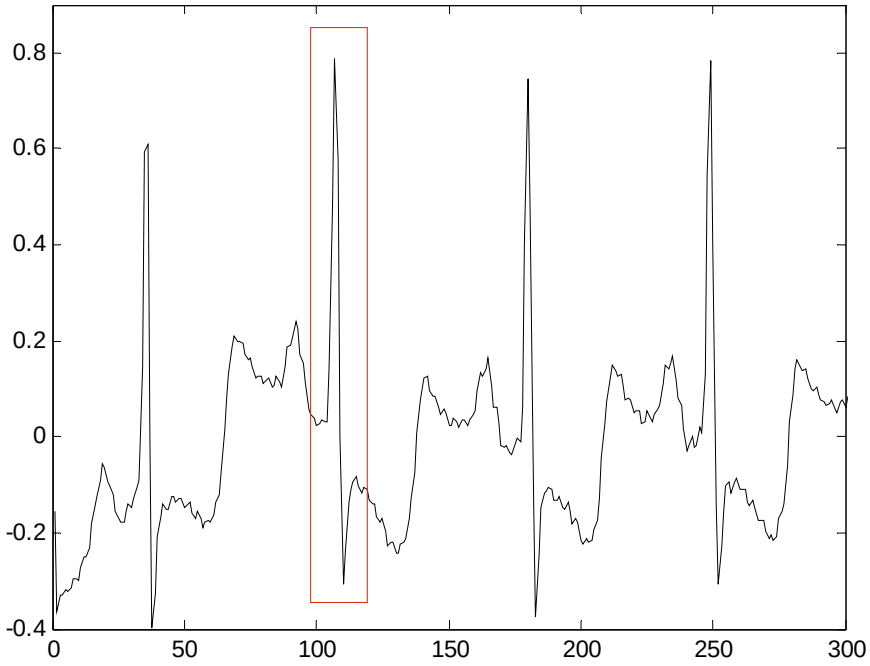

Figure 3.28 200 ms sliding window to be feed to the input layer

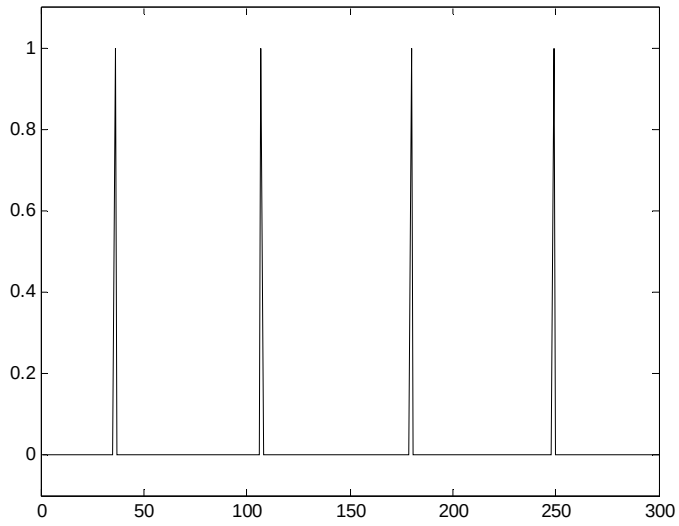

Figure 3.29 Target output for the ECG signal in Figure 3.28

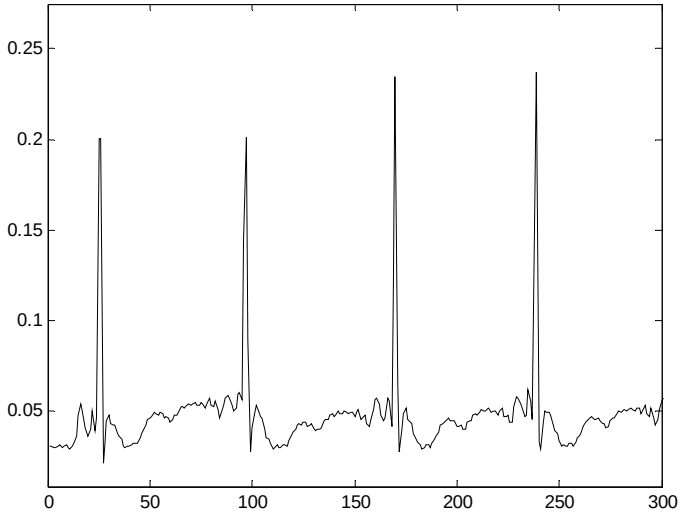

Figure 3.30 Actual output for the ECG data in Figure 3.28

3.3 Feature Extraction and Classification

After the QRS complexes are detected, certain features are extracted from the ECG signal. These features are then used in classification algorithms to differentiate normal beats from the abnormal ones. Extracted features and classification methods implemented in this thesis are provided in the following sections.

3.3.1 Feature Extraction

In this thesis, 16 morphological features are extracted from the detected QRS complexes. In order to achieve this, first some reference points are extracted. These reference points are the positive peak, the negative peak, the onset and the offset points as depicted in Figure 3.31.

The positive peak of the pattern is the maximum point and the negative peak is the minimum point within the QRS complex. Onset of the identified pattern is defined as the local minimum around the point at which the sign of slope is changed prior to the positive peak. Offset of the identified pattern is set to the point having the same amplitude with the onset point after the negative peak.

16 morphological features derived from these reference points are described in Table 3.1 and some of them are illustrated in Figure 3.31. The features numbered from 1 to 12 are taken from [35]; the features numbered from 13 to 16 are original contributions of this thesis.

Table 3.1 Morphological features derived from detected QRS complexes

Number	**Label**	**Description**
1	Pp	Maximum amplitude of positive peak
2	Pn	Maximum amplitude of negative peak
3	Width	The time-interval between the onset and the offset of the identified pattern
4	ArP	Area between the line passing through the onset and offset points and the samples above this line
5	ArN	Area between the line passing through the onset and offset points and the samples below this line
6	Area	Total area of the QRS complex (ArP+ArN)
7	No	Number of samples crossing 70% of the amplitude difference between Pp and Pn
8	Ima	Time interval from QRS complex onset to positive peak.
9	Imi	Time interval from QRS complex onset to negative peak.
10	S1	QRS slope calculated for the time-interval between the QRS complex onset and the first peak (Pp/Ima)
11	S2	QRS slope calculated for the time-interval between positive peak and negative peak (Np /(Imi-Ima))

Table 3.1 (continued) Morphological features derived from detected QRS complexes

Number	Label	Description
12	Pp_dif	Time interval between the occurance of Pp of the identified pattern and the occurance of Pp of the previous pattern
13	Pp_ ratio	The ratio between the Pp_dif of the identified pattern and the next pattern
14	S3	QRS slope calculated for the time-interval between Pn and offset (Pn /(Offset_time-Np_time))
15	Amp_ratio	Ratio of positive peak amplitude and negative peak amplitude (Pp/Pn)
16	Area_ratio	Ratio of positive area and negative area (Parea/Narea)

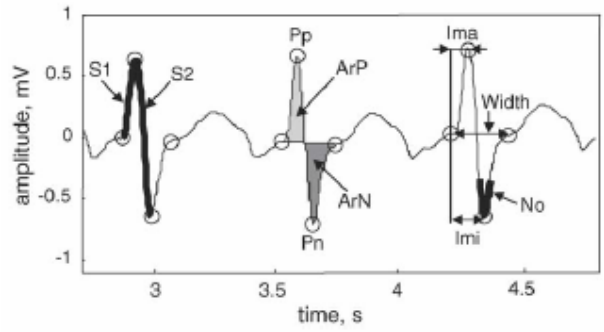

Figure 3.31 Morphological features extracted from detected QRS complexes [35]

3.3.2 Classification

Three classification algorithms are implemented in this study. These are:

- (Classification Method I) K-th nearest neighbour rule,
- (Classification Method II) Artificial neural network,
- (Classification Method III) Rule based classification.

These classification algorithms are explained in the following sections.

3.3.2.1 Classifcation Method I

In this method, Kth nearest neighbor rule is implemented [34] in order to classify normal and PVC beats. This rule operates in a multidimensional space classifying the n-dimensional feature set of an ECG beat based on the nearest points with known correct classification, in the feature space.

The heartbeats are presented by n-dimensional vectors of features. Various combinations of features are applied to the training data set in order to achieve the optimal feature set which is found to be: x = {Pp, Pn, Width, ArN, Area, Ima, Imi, Pp_dif, Pp_ ratio, Area_ratio}. The reference sets composed of Normal and PVC classes are formed from the first 80 seconds of the MITDB records 105 MDII and 122 MDII. Each vector was previously labelled as belonging to one of the three classes by the database signal annotations. A new vector x (with unknown classification) is classified on the basis of the nearest vector from the used reference set. The distance between the vector x and each of the clusters z^j is computed as Euclidean distance to the mean vector of the corresponding cluster:

$$d_j = \sqrt{\sum_{i=1}^{n} \left(x_{i-norm} - z_i^j \right)^2} \qquad (2.22)$$

where j is the cluster index, i is the parameter index, and n is number of the features

used. Vector x is classified as belonging to the class of the cluster z^j at which d_j has a minimum. All features used in this equation is previously scaled so that they take on values ranging from 0 to 1 so that their different magnitudes do not yield unequal weights in the calculation of z^j.

3.3.2.2 Classifcation Method II

In this algorithm [34], classification of normal, PVC and paced beats are performed by a MLP network of two layers. The activation function is described by a sigmoid function ranging from 0 to 1.

Various combinations of features are applied to the input layer in order to achieve the optimal feature set which is found to be: x = {Pp, Pn, Width, ArN, Area, Ima, Imi, Pp_dif, Pp_ ratio, Area_ratio}, The reference sets composed of Normal and PVC classes are formed from the first 80 seconds of the MITDB records 105 MDII and 122 MDII. Each vector was previously labelled as belonging to one of the three classes by the database signals annotations. The number of nodes in the hidden layers are determined experimentally until the best results are obtained. There are 10 nodes in the input layer, 4 neurons in the hidden layer and 1 node at the output layer. The target vector at the output is set to 0.999 if the "Normal" input is fed into the network; and it is 0.001 if a "PVC" input is fed into the network.

After the training process is completed, test set is passed through the network. Threshold stage is applied to the signal at the output node in order to classify normal and PVC beats.

3.3.2.3 Classifcation Method III

The classification approach suggested by Tompkins [5] is a rule based algorithm utilizing a map of QRS duration and RR interval.

R wave is the absolute maximum point within the QRS complex. RR interval is calculated from the time differences of the occurrences of consecutive QRS

complexes. QRS duration is calculated from the time difference between the occurrences of Q and S waves of the detected QRS complexes. Q wave is the first inflection point prior to R wave. Q wave is recognized by a change in the sign of slope. S wave is the first inflection point after R wave. Similar to Q wave recognition, S wave is recognized by a change in the sign of the slope.

In the mapping, a "Normal" region is set by allowing the algorithm to learn with the first 8 normal complexes. These 8 complexes are verified by the annotations in MIT-BIH database. After the learning process, boundaries of "Normal" region are defined in the two-dimensional mapping space as illustrated in Figure 3.32.

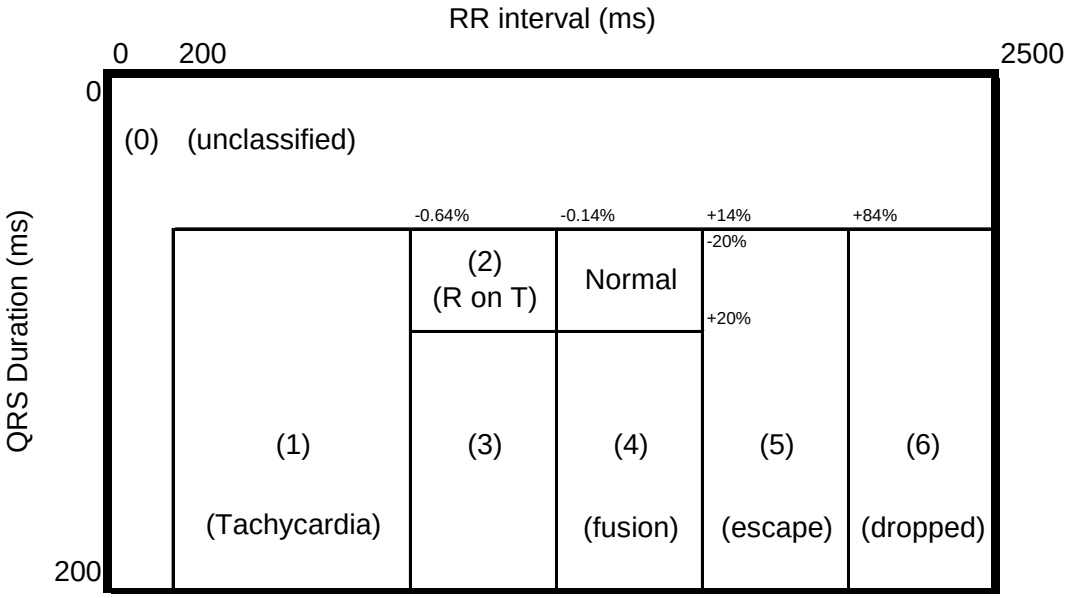

Figure 3.32 Rule based classification algorithm [5]

Except for region "0", boundaries of the other regions are set as the percentages of the mean value of the normal region. Boundaries of region "0" are set according to physiological limits. Region "0" covers physiologically impossible RR intervals or QRS durations. Therefore, any point that falls in region "0" is taken as noise.

The boundaries of the regions are updated according to average RR interval of the most recent 8 beats which are classified as normal. Therefore, the algorithm adapts

itself to changes in heart rate, which may arise from physical exercise etc. According to these defined regions, criteria used for classification of different arrhythmias are described in Table 3.2.

Table 3.2 Criteria used for classification of different arrhythmias based on QRS duration and RR interval

Classification	**Criteria**
Normal	A beat in the normal region.
Asystole	No R wave for more than 1.72 s; less than 35 beats/min.
Dropped	A long RR interval; beat in region 6.
R on T	A beat in region 2.
Compansated PVC	A beat in region 3, followed by another in region 5.
Uncompanseted PVC	A beat in region 3, followed by another in the normal region.
Couplet	Two consecutive beats in region 3 followed by a beat in the normal region, or in region 5.
Paroxysmal Bradcardia	At least three consecutive beats in region 5.
Tachycardia	Average RR interval is less than 0.5 sec.
Fusion	A beat in region 4.
Escape	A beat in region 5.
Rejected	A beat in region 0. (Beat has an RR interval of 200 ms or less, or QRS duration of 60 ms or less)

CHAPTER 4

PERFORMANCE EVALUATION

The tests performed in this study are performed on the first 80s of the records with sampling frequency of 360 sps, in MIT-BIH database. The results are provided in the following sections.

4.1 QRS Complex Detection

In this thesis, developed algorithms for QRS complex detection are tested on records containing normal sinus rhythm, paced rhythm, transition from paced to normal sinus rhythm, noise in lower signal, fusion PVC, first degree AVB, PVC, atrial fibrillation, APC, right bundle branch block, left bundle branch block beats. Since some records are used for training, the test set of method IV is smaller than the others. Initially, each recording is prefiltered as described in section 3.1, and then the QRS detection methods are applied to the prefiltered signal.

The test results of QRS detection methods are provided in Table 4.1, Table 4.2, Table 4.3 and Table 4.4.

When Method I was used for QRS detection, there were four false negatives (i.e., QRS beats that were missed by the algorithm), and four false positives (i.e., parts of the ECG signal other than the QRS region that were falsely detected as a QRS beat). QRS detection of Method I is based on extracting relatively higher frequency content of QRS complex by differentiation. The type of the QRS beats that are missed by Method I have depressed ST segments and lower R peaks and the false positives are usually noisy regions of the ECG signal. Even though prefiltering is applied to the ECG signal, it is observed that Method I has the highest noise sensitivity among all other algorithms. A typical example of beat types which Method I fails to detect is

provided in Figure 4.1. In this figure, 2nd beat, which has a depressed ST segment is missed because its slope characteristic was under the threshold value. The 6th beat has also depressed ST segment, but the algorithm could detect that beat since its higher R peak amplitude results higher slope characteristic than the 2nd beat. Although decreasing the threshold value might seem to be a solution for detection of the missed 2nd beat, this results in an increase in false positives due to increase in noise sensitivity and a sensitivity for elevated T waves.

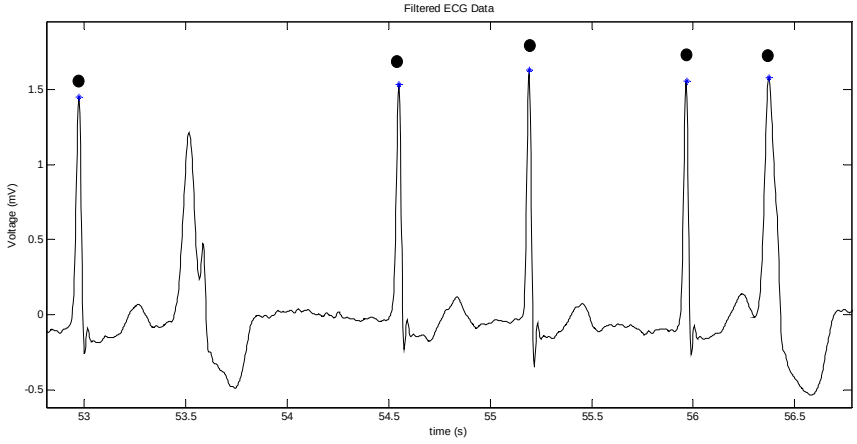

Figure 4.1 An example of false negative with QRS Detection Method I

A typical example of beat types which Method I detects falsely as a QRS beat is provided in Figure 4.2. In this figure, three beats are detected, but the second one is not a beat but a noise. Around this false positive (from about 7.6 s to 7.8 s), the ECG signal changes its slope rapidly. Since this algorithm depends only on the slope characteristic, the portions of the signal with rapid changes in slope such as in this example might be falsely detected as a QRS complex.

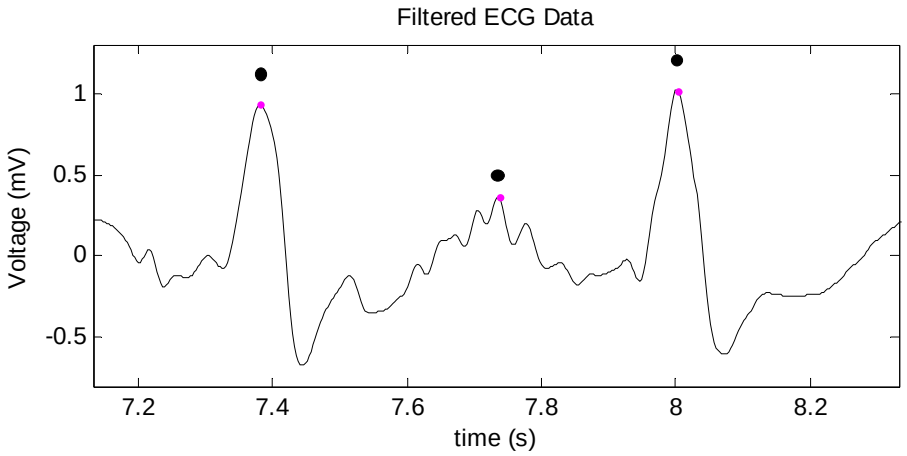

Figure 4.2 An example of false positive with QRS Detection Method I

When Method II was used for QRS detection, there were nine false negatives, and no false positives. QRS detection of Method II is based on digital filtering. The type of the QRS beats that are missed by Method II have depressed ST segments in such a way that the negative area (usually the area between the baseline and the depressed ST segment) and the positive area (usually the area between the baseline and R peak peripheral) cancel each other during the moving average step in Method II. A typical example of beat types which Method I fails to detect is provided in Figure 4.3. In this figure, 2nd beat is missed because the area below the baseline and the area above the baseline cancel each other during moving average filtering step. Method II tends to miss the detection of this type of beats more than detecting extra beats; the number of false negatives is quite high although there are no false positives. This results in decrease in sensitivity with high positive predictivity, which is consistent with the results of [6]. According to the comparison made by [6], this method was found to be one of the best ones among others in terms of false positive detections. In that study, this method did not yield false positives in case of respiration, powerline interference, composite noise corrupted signal. However, in case of high EMG (ranging from DC. to 10 kHz) or baseline shift (ranging from 0.15 Hz. to 0.3 Hz) corruption (for noise levels above %75), this algorithm gave false positives. The band passed filter implemented in this study suppresses baseline shift and some portions of EMG noise

such that no false positives were detected in our results.

Method II has better performance than Method I in terms of the total number of the false positives meaning that it is not sensitive to noise. However, it is unable to detect some pathologic beats as described above.

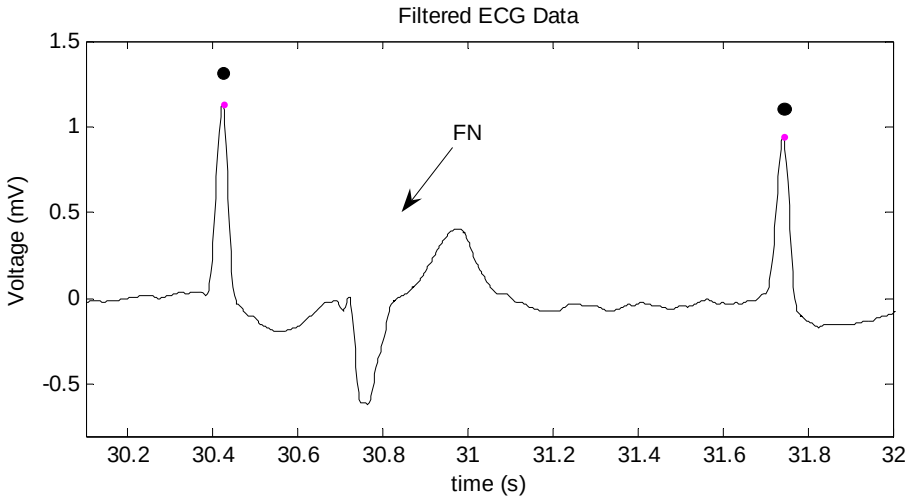

Figure 4.3 An example of false negative with QRS Detection Method II

When Method III was used for QRS detection, there were three false negatives, and no false positives. QRS detection of Method III is based on extracting slope, amplitude and duration characteristics of the QRS complex. The types of the QRS beats that are missed by Method III have very low R amplitudes. A typical example of beat types which Method I fails to detect is provided in Figure 4.4. In this figure, 2nd beat is missed because it has very low amplitude, lower slope and duration. Although lowering the threshold value might seem to be a solution for detection of such missed beats, this results in an increase in false positives due to increase in noise sensitivity and a sensitivity for elevated T waves.

After testing Method III with prefiltering stage described in section 3.1, another test is performed with Method III without this prefiltering stage. Same results were obtained

as expected since Method III has its own filtering stage within the algorithm. The cascaded filtering stages within Method III maximizes the QRS energy within approximately 5-15 Hz. range so that QRS detection stages within Method III are able to operate on 10 Hz at which the maximum SNR exists for QRS complex.

By employing slope, amplitude and width information combined with the embedded prefiltering stages, Method III has the best performance among all the other algorithms.

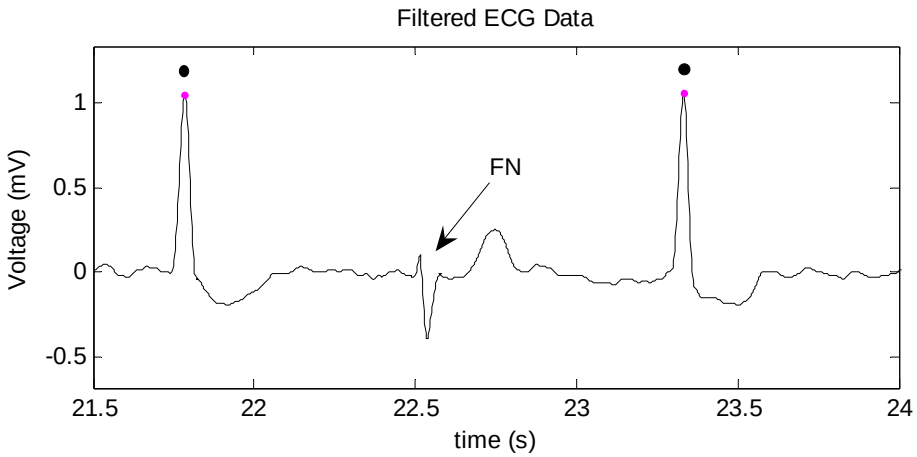

Figure 4.4 An example of false negative with QRS Detection Method III

When Method IV was used for QRS detection, there were 28 false negatives, and five false positives. QRS detection of Method IV is based on neural networks. Due to the perceptron convergence procedure Method IV, performance decreases, for the regions at which the distributions of the classes (a QRS complex or not a QRS complex) overlap. It is difficult to make a visual generalization of these overlapped regions. However, it is observed that this method fails to detect some pathological beats such as the ones with negative R wave. A typical example of beat types which Method IV fails to detect is provided in Figure 4.5. In this figure, 2nd beat with as abnormal negative R peak is missed. A typical example of beat types that Method IV detects falsely as a QRS beat is provided in Figure 4.6. In this figure, 2nd beat has elevated T wave, which is falsely detected as a QRS complex by this algorithm. The effect of

further training in order to improve the performance of the algorithm is expected to oscillate the decision boundary only; resulting in no improvements in performance.

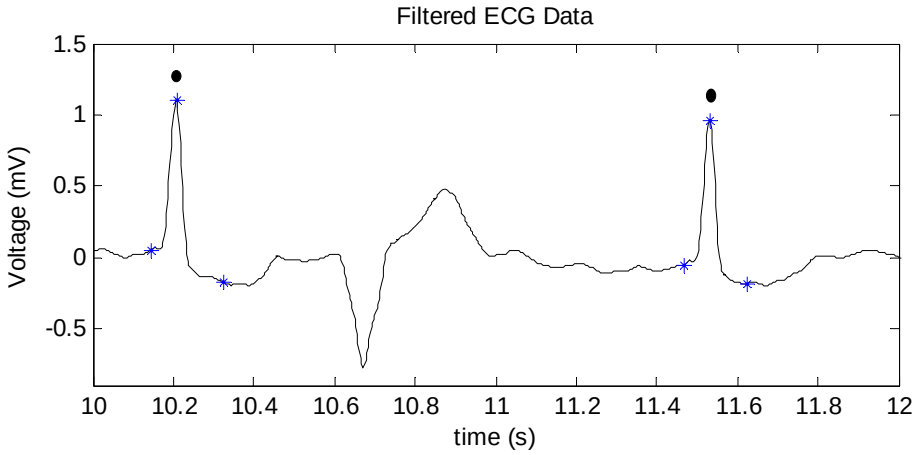

Figure 4.5 An example of false negative with QRS Detection Method IV

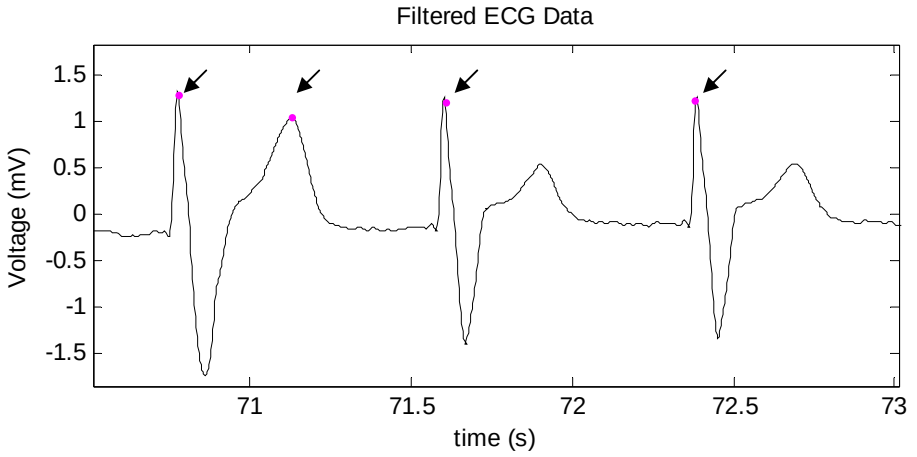

Figure 4.6 An example of false positive with QRS Detection Method IV

Table 4.1 .Test results of QRS complex detection method I

Record	TP	FN	FP	Se	+P
MITDB 100 MDII	95	0	0	100.00	100.00
MITDB 100 V5	95	0	0	100.00	100.00
MITDB 102 V5	93	0	0	100.00	100.00
MITDB 102 V2	102	0	0	100.00	100.00
MITDB 103 MDII	95	0	0	100.00	100.00
MITDB 103 V2	95	0	0	100.00	100.00
MITDB 105 MDII	106	0	0	100.00	100.00
MITDB 106 MDII	92	0	0	100.00	100.00
MITDB 107 MDII	101	0	0	100.00	100.00
MITDB 109 MDII	113	0	3	100.00	97.41
MITDB 111 MDII	96	0	0	100.00	100.00
MITDB 112 MDII	119	0	0	100.00	100.00
MITDB 112 V1	116	0	0	100.00	100.00
MITDB 113 MDII	80	0	0	100.00	100.00
MITDB 114 MDII	76	0	0	100.00	100.00
MITDB 115 MDII	87	0	0	100.00	100.00
MITDB 117 MDII	69	0	0	100.00	100.00
MITDB 118 MDII	100	0	0	100.00	100.00
MITDB 119 MDII	91	0	0	100.00	100.00
MITDB 119 V1	100	0	0	100.00	100.00
MITDB 121 MDII	84	0	1	100.00	98.82
MITDB 122 MDII	121	0	0	100.00	100.00
MITDB 123 MDII	69	0	0	100.00	100.00
MITDB 124 MDII	69	0	0	100.00	100.00
MITDB 201 MDII	125	0	0	100.00	100.00
MITDB 202 MDII	73	0	0	100.00	100.00
MITDB 205 MDII	123	0	0	100.00	100.00
MITDB 209 MDII	129	2	0	98.47	100.00
MITDB 210 MDII	126	0	0	100.00	100.00
MITDB 212 MDII	125	0	0	100.00	100.00
MITDB 213 MDII	153	0	0	100.00	100.00
MITDB 215 MDII	158	0	0	100.00	100.00
MITDB 217 MDII	100	0	0	100.00	100.00
MITDB 219 MDII	105	0	0	100.00	100.00
MITDB 221 MDII	108	1	0	99.08	100.00
MITDB 223 MDII	110	1	0	99.10	100.00
MITDB 230 MDII	108	0	0	100.00	100.00
MITDB 231 MDII	88	0	0	100.00	100.00
MITDB 234 MDII	128	0	0	100.00	100.00
Total	4023	4	4	99.90	99.90

Table 4.2 .Test results of QRS complex detection method II

Record	TP	FN	FP	Se	+P
MITDB 100 MDII	95	0	0	100.00	100.00
MITDB 100 V5	95	0	0	100.00	100.00
MITDB 102 V5	93	0	0	100.00	100.00
MITDB 102 V2	102	0	0	100.00	100.00
MITDB 103 MDII	95	0	0	100.00	100.00
MITDB 103 V2	95	0	0	100.00	100.00
MITDB 105 MDII	106	0	0	100.00	100.00
MITDB 106 MDII	92	0	0	100.00	100.00
MITDB 107 MDII	101	0	0	100.00	100.00
MITDB 109 MDII	110	0	0	100.00	100.00
MITDB 111 MDII	96	0	0	100.00	100.00
MITDB 112 MDII	119	0	0	100.00	100.00
MITDB 112 V1	116	0	0	100.00	100.00
MITDB 113 MDII	80	0	0	100.00	100.00
MITDB 114 MDII	76	0	0	100.00	100.00
MITDB 115 MDII	87	0	0	100.00	100.00
MITDB 117 MDII	69	0	0	100.00	100.00
MITDB 118 MDII	100	0	0	100.00	100.00
MITDB 119 MDII	91	0	0	100.00	100.00
MITDB 119 V1	100	0	0	100.00	100.00
MITDB 121 MDII	83	0	0	100.00	100.00
MITDB 122 MDII	121	0	0	100.00	100.00
MITDB 123 MDII	69	0	0	100.00	100.00
MITDB 124 MDII	69	0	0	100.00	100.00
MITDB 201 MDII	124	1	0	99.20	100.00
MITDB 202 MDII	73	0	0	100.00	100.00
MITDB 205 MDII	123	0	0	100.00	100.00
MITDB 209 MDII	131	0	0	100.00	100.00
MITDB 210 MDII	121	5	0	96.03	100.00
MITDB 212 MDII	125	0	0	100.00	100.00
MITDB 213 MDII	153	0	0	100.00	100.00
MITDB 215 MDII	158	0	0	100.00	100.00
MITDB 217 MDII	100	0	0	100.00	100.00
MITDB 219 MDII	105	0	0	100.00	100.00
MITDB 221 MDII	108	1	0	99.08	100.00
MITDB 223 MDII	109	2	0	98.20	100.00
MITDB 230 MDII	108	0	0	100.00	100.00
MITDB 231 MDII	88	0	0	100.00	100.00
MITDB 234 MDII	128	0	0	100.00	100.00
Total	4014	9	0	99.78	100.00

Table 4.3 .Test results of QRS complex detection method III

Record	TP	FN	FP	Se	+P
MITDB 100 MDII	95	0	0	100.00	100.00
MITDB 100 V5	95	0	0	100.00	100.00
MITDB 102 V5	93	0	0	100.00	100.00
MITDB 102 V2	102	0	0	100.00	100.00
MITDB 103 MDII	95	0	0	100.00	100.00
MITDB 103 V2	95	0	0	100.00	100.00
MITDB 105 MDII	106	0	0	100.00	100.00
MITDB 106 MDII	92	0	0	100.00	100.00
MITDB 107 MDII	101	0	0	100.00	100.00
MITDB 109 MDII	110	0	0	100.00	100.00
MITDB 111 MDII	96	0	0	100.00	100.00
MITDB 112 MDII	119	0	0	100.00	100.00
MITDB 112 V1	116	0	0	100.00	100.00
MITDB 113 MDII	80	0	0	100.00	100.00
MITDB 114 MDII	76	0	0	100.00	100.00
MITDB 115 MDII	87	0	0	100.00	100.00
MITDB 117 MDII	69	0	0	100.00	100.00
MITDB 118 MDII	100	0	0	100.00	100.00
MITDB 119 MDII	91	0	0	100.00	100.00
MITDB 119 V1	100	0	0	100.00	100.00
MITDB 121 MDII	83	0	0	100.00	100.00
MITDB 122 MDII	121	0	0	100.00	100.00
MITDB 123 MDII	69	0	0	100.00	100.00
MITDB 124 MDII	69	0	0	100.00	100.00
MITDB 201 MDII	125	0	0	100.00	100.00
MITDB 202 MDII	73	0	0	100.00	100.00
MITDB 205 MDII	123	0	0	100.00	100.00
MITDB 209 MDII	131	0	0	100.00	100.00
MITDB 210 MDII	124	2	0	98.41	100.00
MITDB 212 MDII	125	0	0	100.00	100.00
MITDB 213 MDII	153	0	0	100.00	100.00
MITDB 215 MDII	158	0	0	100.00	100.00
MITDB 217 MDII	100	0	0	100.00	100.00
MITDB 219 MDII	105	0	0	100.00	100.00
MITDB 221 MDII	109	0	0	100.00	100.00
MITDB 223 MDII	110	1	0	99.10	100.00
MITDB 230 MDII	108	0	0	100.00	100.00
MITDB 231 MDII	88	0	0	100.00	100.00
MITDB 234 MDII	128	0	0	100.00	100.00
Total	4020	3	0	99.93	100.00

Table 4.4 .Test results of QRS complex detection method IV

Record	TP	FN	FP	Se	+P
MITDB 100 V5	95	0	0	100.00	100.00
MITDB 102 V5	93	0	0	100.00	100.00
MITDB 102 V2	102	0	0	100.00	100.00
MITDB 103 MDII	95	0	0	100.00	100.00
MITDB 103 V2	95	0	0	100.00	100.00
MITDB 105 MDII	101	5	0	95.28	100.00
MITDB 106 MDII	92	0	0	100.00	100.00
MITDB 107 MDII	105	0	4	100.00	96.33
MITDB 109 MDII	110	1	0	99.10	100.00
MITDB 111 MDII	96	0	0	100.00	100.00
MITDB 112 MDII	119	0	0	100.00	100.00
MITDB 112 V1	116	0	0	100.00	100.00
MITDB 113 MDII	81	0	1	100.00	98.78
MITDB 114 MDII	76	0	0	100.00	100.00
MITDB 115 MDII	87	0	0	100.00	100.00
MITDB 117 MDII	69	0	0	100.00	100.00
MITDB 118 MDII	100	0	0	100.00	100.00
MITDB 121 MDII	83	0	0	100.00	100.00
MITDB 122 MDII	121	0	0	100.00	100.00
MITDB 123 MDII	69	0	0	100.00	100.00
MITDB 124 MDII	69	0	0	100.00	100.00
MITDB 201 MDII	125	11	0	91.91	100.00
MITDB 202 MDII	73	0	0	100.00	100.00
MITDB 205 MDII	123	0	0	100.00	100.00
MITDB 209 MDII	130	1	0	99.24	100.00
MITDB 210 MDII	126	7	0	94.74	100.00
MITDB 212 MDII	125	0	0	100.00	100.00
MITDB 219 MDII	103	2	0	98.10	100.00
MITDB 221 MDII	109	0	0	100.00	100.00
MITDB 223 MDII	110	1	0	99.10	100.00
MITDB 230 MDII	108	0	0	100.00	100.00
MITDB 231 MDII	88	0	0	100.00	100.00
MITDB 234 MDII	128	0	0	100.00	100.00
Total	3322	28	5	99.16	99.85

The performances of the algorithms in literature which form the starting points of the algorithms implemented in this thesis and comparison of the results obtained in this thesis are provided in the following paragraphs. A direct comparison between our

results and those taken from the literature may not be possible since the datasets on which the algorithms are tested are not the same. However, the following discussions would still be valuable to assess the overall performances of the algorithms implemented in this thesis among each other.

In [6], the authors tested Method I and Method II with synthesized noise composed of EMG, power line, respiration and baseline shift artifacts, and observed that for Method I sensitivity and positive predictivity have decreased to 70.00% and 77.78 % respectively when tested with 25 percent noise. For Method II, sensitiviy and positive predictivity are 95.00% and 100.00% respectively, even with 75% noise.

In [12], it was found that that the sensitivity and positive predictivity of Method III are 99.68% and 99.63% respectively when tested on MIT-BIH database with datasets different from those used in this thesis.

In [2], it is reported that sensitivity and positive predictivity of algorithms similar to Method IV are greater than 99% when tested with some parts of MIT-BIH database.

The summary of overall test results of QRS detection methods of this thesis are provided in Table 4.5. Since the parameters in the algorithms are very well tuned to this dataset in order to obtain the best results, there is a possibility for their performances to decrease when tested with different datasets.

Direct comparison of the results of Method I and II with the corresponding ones in literature is not reasonable since prefiltering stage is applied in this thesis however the ones in the literature are tested directly in noisy data sets. However in literature it is observed that noise sensitivity of Method I is higher that Method II and Method II tends to miss beats more than detecting extra beats (number of false negatives are greater than false positives) which are consistent with the results obtained in this study.

Since the data sets used in the literature are not the same for Method III and IV, direct comparison of the results of this study with the corresponding ones in the literature is

not possible. However, there is no major difference in between the overall results of this study and the results in literature; therefore, one can say that the results observed in this thesis and the results reported in previous publications are in agreement in the general sense.

Table 4.5 .Over all test results of QRS complex detection methods

Record	TP	FN	FP	Se	+P
Method I	4023	4	4	99.90	99.90
Method II	4014	9	0	99.78	100.00
Method III	4020	3	0	99.93	100.00
Method IV	3322	28	5	99.16	99.85

4.2 Feature Extraction and Classification

After QRS complex detection by Method III which has the best results among the other detection algorithms as mentioned in the previous section, the reference sets composed of Normal and PVC beats formed by the first 80 second of the MITDB records 105 MDII and 122 MDII are utilized in classification Methods I and II. Statistical assessment (median value, 25–75% range around the median value and min–max range) of sixteen morphological features, in groups defined by the two major heartbeat classes (i.e., normal and PVC classes) are depicted in Figure 4.7. Those features whose statistical distributions for normal and PVC beats do not overlap are considered to have superior discrimination capability than the ones whose statistical distributions overlap for normal and PVC clusters. With this criterion in mind, discrimination property of the following set is observed to be superior than the others: {Width, ArN, Area, Imi, Pp_dif, Pp_ratio, ArP,}. Within this set, it is observed that the feature {Parea} seems to be dependent on the other features in a way that absence of this feature in the set did not decrease the performance. Therefore, feature {ArP} is not used for classification. Additionally, although discrimination property of the features of the set {Pp, Pn, Ima, Area_ratio} seems to be poor, it is observed that their existence in the set improved the performance when they are used jointly with the selected feature set. Therefore, the optimal set of the features as being {Pp, Pn, Width, ArN, Area, Ima, Imi, Pp_dif, Pp_ratio, Area_ratio}

are obtained in an empirical way based on the trial of combinations of the features.

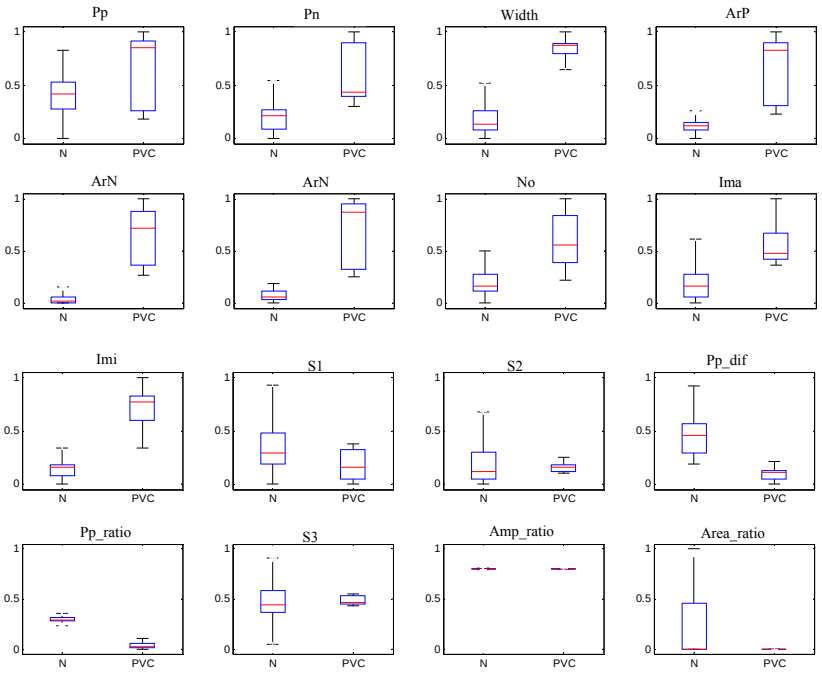

Figure 4.7 Statistical assessment (median value, 25–75% range around the median value and min–max range) of sixteen morphological features, in groups defined by the different heartbeat classes.

In order to test the classification algorithms I and II, the records containing only normal and PVC beats are used which are: 106 MDII, 119 MDII, 221 MDII, 115 MDII, 121 MDII, 123 MDII. These records contain 489 normal and 42 PVC beats.

Sensitivity measure is used to assess the performance of the classification algorithms. The sensitivity measure evaluates the proportion of PVC beats that are correctly identified as PVC. In this study, PVC beats correctly classified as PVC are referred to as true positive (TP), normal beats correctly classified as normal are referred to as true negative (TN), normal beats wrongly classified as PVC are referred to as false positive (FP) and PVC beats wrongly classified as normal are referred to as false negative (FN).

Sensitivities for Method I and Method II are 92.86% and 95.24% respectively as

provided in Table 4.6. The results of both algorithms are comparable with the ones in the literature. For normal and PVC beats, [34] implemented classification methods similar to Method I and Method II. For three different datasets, obtained sensitivity values between 80.9% to 96.9% for a method similar to Method I, and between 80.7% to 97.7% for a method similar to Method II.

Table 4.6 .Test results for classification Method I and Method II

Method	# of TP	# of TN	# of FP	# of FN	Sensitivity
Method I	39	475	14	3	92.86%
Method II	40	489	0	2	95.24%

Method III is assessed separately from Method I and Method II, because the type of beats classified with Method III are more diverse than those of the first two methods. For method III, classification results did not match very well with the MIT-BIH database annotations. An example of classification results with Method III and the MIT-BIH database annotations respectively for the same beat sequence are depicted in Figure 4.8 and Figure 4.9. Method III classifies this beat sequence as being "normal, normal, tachycardia, tachycardia, escape, normal, fusion, normal, normal, fusion" consequently. However, this beat sequence is annotated as being "normal, normal, PVC, PVC, normal, normal, normal, normal, normal, normal" by MIT-BIH database.

In MIT-BIH database only the occurrence of beats and the associated pathologies are annotated but not the Q and S waves which are used to calculate the duration of the QRS complex. Therefore, a study has been carried out with a cardiologist, Prof. Dr. Nazım ARSLAN, over typical examples of detected Q and S waves. Dr. Arslan stated that although for the normal beats Q and S points are located correctly, for some pathological beats the algorithm fails to locate the waves correctly.

For example, the algorithm correctly detects the Q, R and S waves for the sample beat depicted in Figure 4.10. However, for the second beat in Figure 4.11, the algorithm locates the S wave, to the point depicted with second red circle although the correct location declared by the cardiologist is the one marked with blue circle. The Q wave depicted in Figure 4.12 is located by the algorithm as the green point however the correct location declared by the cardiologist is the one marked with the blue circle.

Method III relies on correct definition of Q and S points, since the QRS duration is one of the two main features in this classification algorithm. When these points are estimated incorrectly, the performance of this algorithm drops, as we have observed in this study.

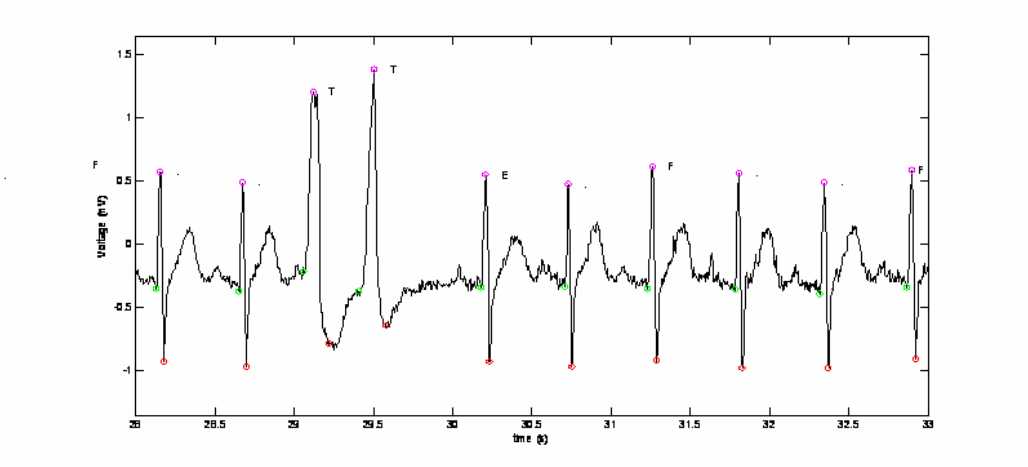

Figure 4.8 An example of classification with Method III (“.”:Normal, “T” Tachycardia,“E”:Escape, “F”:Fusion)

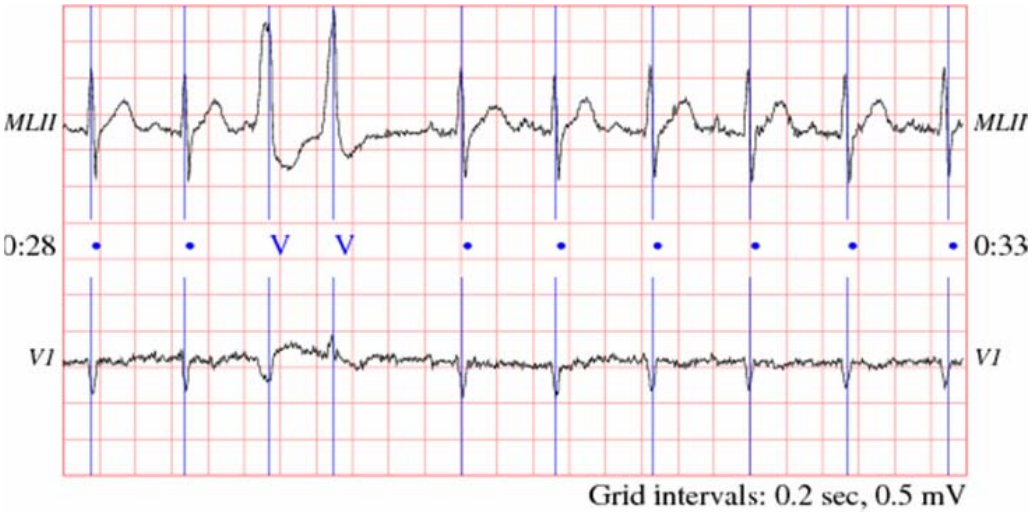

Figure 4.9 MIT-BIH classification for the same signal in Figure 4.9 (“ . ”: Normal, “V”: PVC)

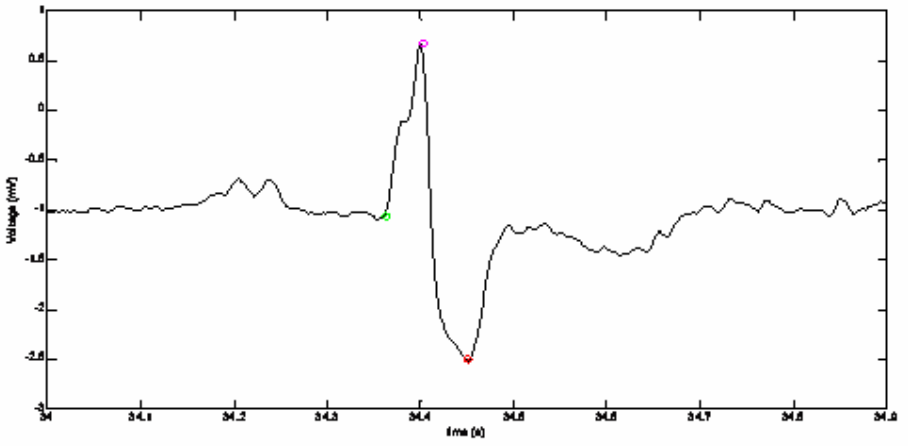

Figure 4.10 A sample beat: detected Q, R and S waves are indicated with circles

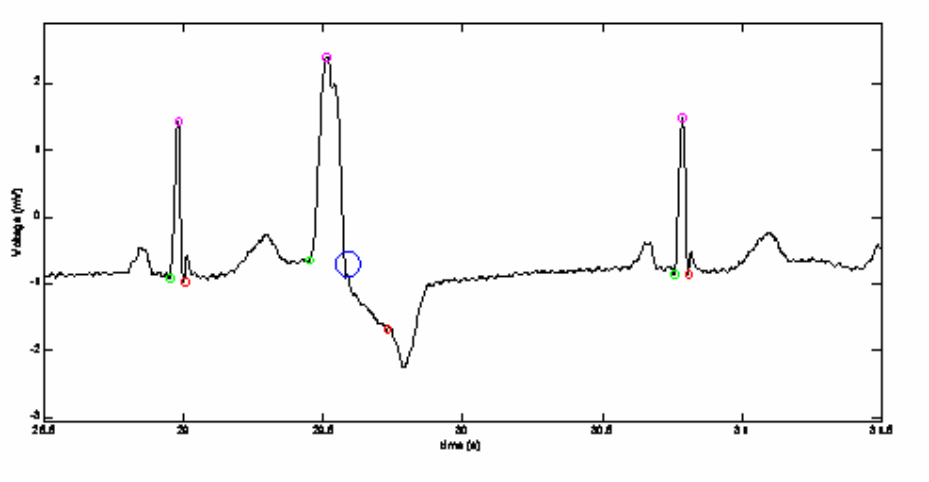

Figure 4.11 An example to a false detection of the S wave: For the second beat the algorithm locates the S wave to the point marked with second red circle although the correct location is the one marked with blue circle.

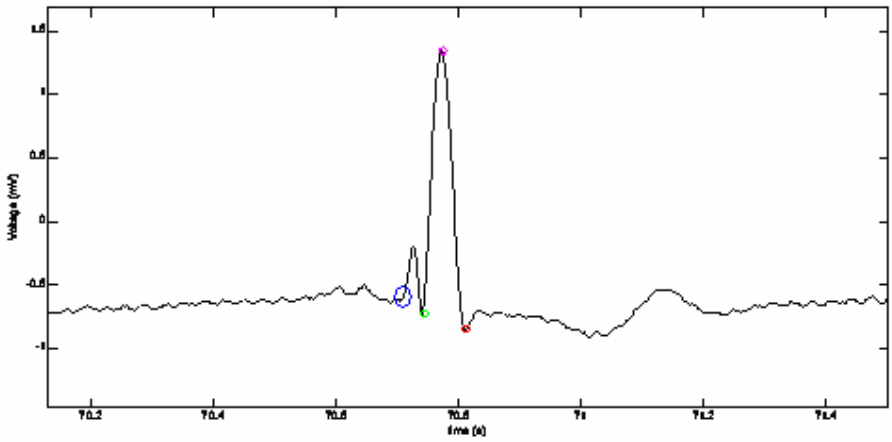

Figure 4.12 An example to a false detection of the Q wave: The algorithm locates the Q wave to the point marked with green circle although the correct location is the one marked with blue circle.

CHAPTER 5

DISCUSSION AND CONCLUSIONS

5.1 Summary and Discussion

ECG is the most important noninvasive tool used for diagnosing the heart diseases. Among several waveforms that exist in an ECG signal, the most important and characteristic one is the QRS complex.

QRS detection is a mature field since most of the algorithms available have been tried and tested on ECG recordings [2] and performances above 99% are achieved without much computational effort [4]. However, in literature, only overall results are provided for detection rates, hiding the problems for individual records having pathological beats and noise corruption [4]. Additionally, many of the algorithms are not tested in a standard database, which makes direct comparison of the algorithms questionable [4].

In this study, for QRS detection four algorithms that are known to be successful are implemented and results are compared. A derivative based method (Method I) [6] and a digital filter based method (Method II) [6] that utilizes the fundamental concepts of QRS detection are implemented. Another method (Method III) [8] that utilizes the morphological features, which is known to be robust and popular by being the most cited reference, is implemented. In addition, a neural network based QRS detection method (Method IV) is implemented, which is reported to be one of the promising techniques as stated in the review chapter of [2]. Sensitivity and positive predictivity measures were used for performance evaluation of the algorithms. The results are given in Tables 4.1, 4.2, 4.3 and 4.4 for ach method, and these results are summarized in Table 4.5. Our observations show that Method III has the best performance.

The disadvantage of Method I is that it is sensitive to noise, yielding an increase in false positives. False positives may be decreased by increasing the threshold value,

but the cost is increase in false negatives. The disadvantage of Method II is that it fails to detect some type of pathologic beats yielding increase in false negatives. The advantage of Method II is that it suppresses non-QRS segments so well that no false positives are observed. Although overall performance indices of Method IV are greater than 99.16% which can be considered to be satisfactory, its individual performance indices decrease to 91.91%, which cannot be acceptable for clinical usage. This method has the worst performance among all other methods. Nevertheless, ANN is still a promising technique as stated in [2] and [4]; ANN methods other than MLP can be considered in order to obtain better results. Method III has the advantage of combining the characteristic features of QRS complex such as amplitude, slope and duration yielding the best overall results among all the tested algorithms.

There is no major difference in between the overall results of this study and the results in literature; therefore, one can say that the results observed in this thesis and the results reported in previous publications are in agreement in the general sense

After detecting the beats by QRS detection Method III, classification of beats are performed. For this purpose, in addition to morphological features suggested by [35], four additional features are extracted. Various combinations of features are applied in a methodic way in order to obtain the optimal feature set. K-th nearest neighbour rule [34] (classification method I) and artificial neural network [34] (classification method II) classification algorithms are implemented in order to classify normal and PVC beats. Although the results are comparable with the similar ones in the literature, performance of these algorithms may decrease in the presence of pathological beats other than PVC.

The rule based classification algorithm [5] (classification method III) implemented in this study utilizes two parameters: RR interval and QRS duration. The results of this algorithm did not match very well with the annotations in MIT-BIH database because the two parameters were not enough to make a global generalization rule and the performance of S point detection method decreases for some pathological beats as

described in section 4.2.

5.2 Conclusions

Among the QRS detection methods tested in this thesis, the best results were obtained with Method III; over 4000 beats were detected with this method, there were no false positives, and only three QRS beats were missed (marked as false negatives). Thus, the overall sensitivity and positive predictivity values of this method are 99.93% and 100%, respectively. Since there were no false positives, the positive predictivity values were 100% for each MIT database record. The three false negatives were observed in two of the records. MITDB 210 MDII had two false negatives and MITDB 223 MDII had only one false negative, yielding sensitivity values of 98.41% and 99.10%, respectively, both of which are acceptable sensitivity values for clinical usage.

Among the tested classification algorithms, the best results were obtained by Method II, which is a neural network based method. Only normal beats and the PVC beats were classified with this method. Out of 489 normal and 42 PVC beats, 40 beats were correctly marked as PVC (true positives), 489 beats were correctly marked as normal beats (true negatives), two PVC beats were incorrectly marked as normal (false negatives). There were no false positives with this classification method. These results produced a sensitivity value of 95.24%.

5.3 Recommendation for Future Work

This section summarizes some future research ideas related to the study presented in this thesis. Some of the future work suggestions are:

- A more detailed study could be carried out on soft computing techniques for QRS detection, for example by employing back search algorithms for offline detection [4].
- More research could be done on extracting waveforms other than QRS complex

and classification by including more pathological beats. Additional algorithms can be implemented for this purpose.

- Neural network methods other than MLP could be considered to increase the performance of the NN based QRS detection algorithm.
- Neural network algorithms could be studied more in order to utilize both detection and classification within one algorithm.

REFERENCES

[1] Malmivuo J. and Plonsey R., “Bioelectromagnetism," Oxford University Press. http://butler.cc.tut.fi/~malmivuo/bem/bembook/index.htm, last accessed on 01.11.2008.

[2] Begg R.,Lai D.T.H., and Palaniswami M., “Computational Intelligence in Biomedical Engineering”, CRC Press, 2008

[3] Tanrıverdi V., “Removal of Baseline Wandering from the Electrocardiogram”, MS Thesis, METU, 2006

[4] Köhler, B., Henning, C., Orglmeister R., “The Principles of Software QRS Detection”, IEEE Engineering in Medicine and Biology, January/February 2002.

[5] Tompkins, W.J., “Biomedical Digital Signal Processing”, Prentice Hall, 1993.

[6] Friesen G.M., Jannett T.C., Jadallah M.A., Yates S.L., Quint S.R., and Nagle H.T., “A Comparison of the Noise Sensistivity of Nine QRS Detection Algortithms”, IEEE Transaction on Biomedical Engineeering. Vol 37 No. 1. January 1990.

[7] Addison P.S., “Wavelet Transform and the ECG: a review”, Institude of Physics Publishing, 2005.

[8] Rangayyan R.M., “Biomedical Signal Analysis”, IEEE Press, 2002.

[9] Yeh Y.C., Wang W.J., “QRS Complexes Detection for ECG Signal: The Difference Operation Method”, Computer Methods and Programs in Biomedicine, 2008.

[10] Pan J., Tompkins W.J., “A Real Time QRS Detection Algorithm”, IEEE

Trans. Biomed. Eng., vol.32, pp 230-236, 1985.

[11] Hamilton P.S., Tompkins W.J., "Quantitive Investigation of QRS Detection Rules Using the MIT/BIH Arrhythmia Database", IEEE Trans. Biomed. Eng., vol. 33, pp. 1157-1165, 1986.

[12] Arzeno N.M., Deng Z.D., and Poon C.S., "Analysis of First Derivative Based QRS Detection Algorithms", IEEE Trans. Biomed. Eng., vol. 55, No.2, 2008.

[13] Hamilton P., "Open Source ECG Analysis", IEEE, 2002.

[14] Moraes JCTB, Freitas MM, Vilani FN., Costa EV., "A QRS Detection Algorithm Using Electrocardiogram Leads", IEEE, 2002.

[15] Suppappola S. and Sun Y., "Nonlinear Transforms of ECG Signals for Digital QRS Detection: a quantative analysis", IEEE Transactions on Bionedical Engineering 41, 397-400, 1994.

[16] Yu B.C., Liu S., Lee M., Chen C.Y., Chiang B.N., "A Nonlinear Digital Filter for Cardiac QRS Complex Detection", J. Clin. Eng., vol. 10, pp.193-201, 1985.

[17] Hamilton P., and Tompkins W., "Adaptive Matched Filtering for QRS Detection", Proceedings of the 10th Annual International Conference of IEEE Engineering in Medicine and and Biology Society Conference 1, 147-148, 1998.

[18] Dandapat S., and Ray G., "Spike Detection in biomedical Signals Using Midprediction Filter", Medical and Biology Engineering and Computing, 1997.

[19] Mallat S., "A Wavelet Tour of Signal Processing (2nd edition)", New York Acedemic Press, 1999.

[20] Senhadji L., Carrault G., Bellanger J. J. and Passariello G.,"Comparing

Wavelet Transforms for Recognizing Cardiac Patterns" IEEE Trans. Med. Biol. 13 167–73, 1995.

[21] Sahambi J. S., Tandon S. M., and Bhatt R. K. P., "Using Wavelet Transforms for ECG Characterization: An On-Line Digital Signal Processing System", IEEE Eng. Med. Biol. 16 77–83, 1997

[22] Sahambi J. S., Tandon S. M. and Bhatt R. K. P., "Quantitative Analysis of Errors Due to Power-Line Interference and Base-Line Drift in Detection of Onsets and Offsets in ECG Using Wavelets", Med. Biol. Eng. Comput. 35 747–51, 1997

[23] Sahambi J. S., Tandon S. M., and Bhatt R. K. P. "Wavelet Base ST-Segment Analysis", Med. Biol. Eng. Comput. 36 568–72, 1998.

[24] Sivannarayana N., and Reddy D. C., "Biorthogonal Wavelet Transforms for ECG Parameters Estimation", Med. Eng.Phys. 21 167–74,1999.

[25] Li C., Zheng C. and Tai C.,"Detection of ECG Characteristic Points Using Wavelet Transforms", IEEE Trans. Biomed.Eng. 42 21–8, 1995.

[26] Shyu L.Y., Wu Y.H. and Hu W., "Using Wavelet Transform and Fuzzy Neural Network for VPC Detection from the Holter ECG", IEEE Trans. Biomed. Eng. 51 1269–73, 2004.

[27] Martinez J. P., Almeida R., Olmos S., Rocha A. P. and Laguna P., "A Wavelet-Based ECG Delineator: Evaluation on Standard Data Bases", IEEE Trans. Biomed. Eng. 51 570–81, 2004.

[28] Kadambe S,, Murray R., and Boudreaux-Bartels G. F., 'Wavelet Transform-Based QRS Complex Detector", IEEE Trans. Biomed. Eng. 46 838–48, 1999.

[29] Romero L. I., Addison P. S., Reed M. J., Grubb N. R., Clegg G. R., Robertson C. E. and Watson J. N.," Continuous Wavelet Transform Modulus Maxima Analysis of the Electrocardiogram: Beat-to-Beat Characterization and Beat to-

Beat Measurement", Int. J. Wavelets, Multiresolution Inf. Process. 3 19–42, 2005

[30] Hu Y. H., Tompkins W.J., Urrusti J.L., Afonso V. X., "Applications of Artificial Neural Networks for ECG Signal Detection and Classification", J. Electrocardiography, vol. 26 (suppl.), pp. 66-73, 1993.

[31] Xue Q., Hu Y. H., Tompkins W. J., "Neural Network Based Adaptive Matched Filtering for QRS Detection", IEEE Trans. Biomed. Eng., vol. 39, pp. 317-329, 1992.

[32] Gang L., Wenyu Y., Ling L., Qilian Y., Xuemin Y., "An Artificial Intelligence Approach to ECG Analysis", IEEE Eng. in Med. and Biology, May/April 2000.

[33] Reaz M.B.I. and Wei L.S., "Detection of the R wave Peak of QRS Complex Using Neural Network", IEEE, 2004.

[34] Poli R., Cagnoni S., Valli G., "Genetic Design of Optimum Linear and Nonlinear QRS Detectors", IEEE Trans. Biomed. Eng., vol 42, pp. 1137-1141, 1995.

[35] Bortolan G., Jekova I., Christov I., "Comparison of Four Methods for Premature Ventricular Contraction and Normal Beat Clustering", Computers in Cardiology;32:921−924, IEEE, 2005.

[36] Christov I.,Herrero G.G., Krasteva V., Jekova I., Gotchev A., and Egiazarian K., "Comparative Study of Morphological and Time-Frequency ECG Descriptors for Heartbeat Classification", Medical Engineering & Physics 28 876–887, 2006.

[37] Osowski S., Hoai L. Markiewicz T., "Support Vector Machiene-Based Expert System for Reliable Heart Beat Recognition", IEEE Transactions on Biomedical Engineering 51(4), 582-589, 2004

[38] Osowski S., Tran H., "ECG Beat Recognition Using Fuzzy Hybrid Neural Network", IEEE Transaction on Biomedical Engineering 48(11), 1265-1271., 2001

[39] Al Fahoum, A., Howitt I., "Combined Wavelet Transformation abd Radial Bases Neural Networks for Classifiying Life-Threathening Cardiac Arrhythmias", Medical and Biological Engineering and Computing 37(5), 566-573, 1999.

[40] Watrous R., Towell G., "A Patient Adaptive Neural Network ECG Patient Monitoring Algorithm", Computers in Cardiology 1, 229-232, 1995.

[41] Marques J., Goncalves A., Ferreira F., Abreu-Lima C., "Comparison of Artifacial Neural Network Based ECG Classifiers Using Different Feature Types", Computers in Cardiology 1,545-547, 1994.

[42] Zhu K., Noakes P., Green A., "ECG Monitoring with Artificial Neural Networks", Proceedings of the 2nd International Conference on Artificial Neural Networks, 205-209, 1991.

[43] Chow H., Moody G., Mark R., "Detection of Ventricular Ectopic Beats Using Neural Networks", Computers in Cardiology, 659-662, 1992.

[44] Oien G., Bertelsen N., Eftestol T., Husoy J., "ECG Rhythm Classification Using Artificial Neural Networks", IEEE Digital Signal Processing Workshop 1, 514-517, 1996.

[45] Yeap T., Johnson F., Rachniowsky M., "ECG Beat Classification by a Neural Network", Proceedings of the 12th Annual International Conference of the IEEE Engineering in Medicine and Biology Society 1, 1457-1458.

[46] Simon B., Eswaran C., "An ECG Classifier Designed Using Modified Decision Based Neural Networks", Computers and Biomedical Research 30(4), 257-272, 1997.

[47] ANSI/AAMI EC57: Testing and reporting performance results of cardiac rhythm and ST segment measurement algorithms (AAMI Recommended Practice/American National Standard), 1998. Available: http://www.aami.org; Order Code: EC57-293.

[48] Moody, G. B., Mark R. G., "The Impact of the MIT-BIH Arrhythma Database", IEEE Engineering in Medicine and Biology, May/June 2001

[49] "Research Resource for Complex Physiologic Signals", http://www.physionet.org/, last accessed on 01.11.2008.

[50] Bishop C. M., "Pattern Recognition and Machiene Learning", Springer, 2006

[51] Halici, U., "EE 543 Lecture Notes", METU, EE, http://vision1.eee.metu.edu.tr/~halici/courses/543LectureNotes/543index.html, last accessed on 01.11.2008.

Appendix A: Graphical User Interface (GUI)

MATLAB based Graphical User Interface (GUI) is prepared as depicted Figure A.1.

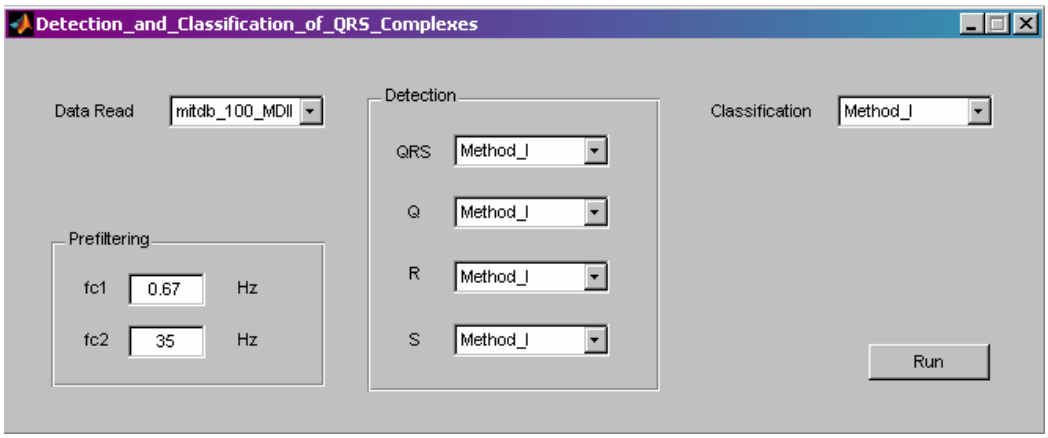

Figure A.1 Graphical user interface

Functions of the objects in the GUI layout are:

- "Data read" menu allows user to choose the ECG data to be processed. Default ECG data is MITDB 100 MDII.

- "Prefiltering" panel allows user to change the default cut off frequencies of the bandpass filter. "fc1" and "fc2" stand for the lower and higher cut off frequencies with 0.67 Hz and 35 Hz as the default values respectively.

- "Detection" panel allows user to choose QRS, Q, R, S detection methods. QRS popup menu includes four different methods as described in the previous sections. Default one for QRS selection is Method I (differentiation method). Pop up menus for Q, R, S detections include only one method for each one which are based on local maximum/minimums are implemented in this thesis. These are implemented as pop up menus in order to allow enhancement of this study in future.

- "Classification" menu allows user to choose the classification methods among the three methods implemented in this thesis. Default one for classification is Method I (KNN method).

- "Run" toggle button starts execution of the functions.

After the toggle button is pressed two windows appear as depicted in Figure A.2 and Figure A.3. The first one is illustrates the unfiltered ECG signal and the second one illustrates the filtered ECG signal, with Q, R, and S points and classification results for each heart beat is indicated. The following abbreviations are used in classification of heart beats: "N": Normal, "PVC": premature ventricular contraction, "uPVC": uncompensated premature ventricular contraction, "C": couplet, "D": dropped, "RT": R on T, "F": Fusion, "E": Escape, "PB": paroxysmal bradcardia, "T": tachycardia, "U": unclassified.

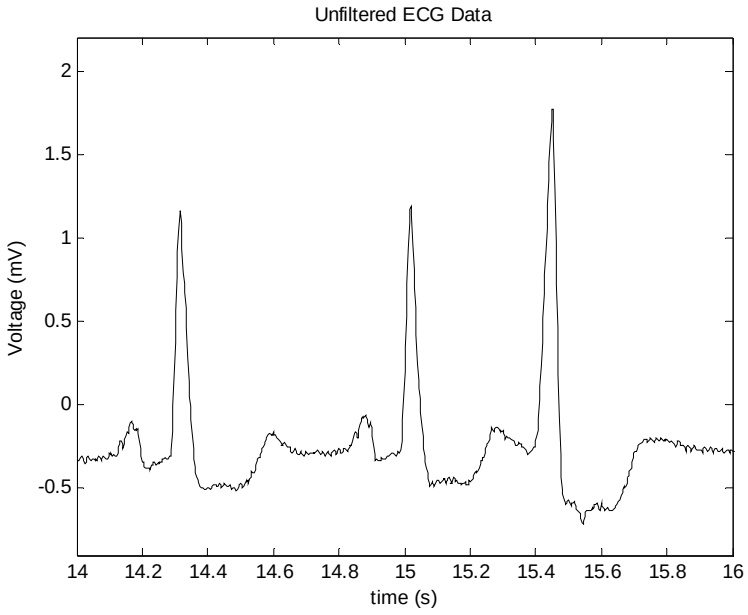

Figure A.2 ECG signal before filtering

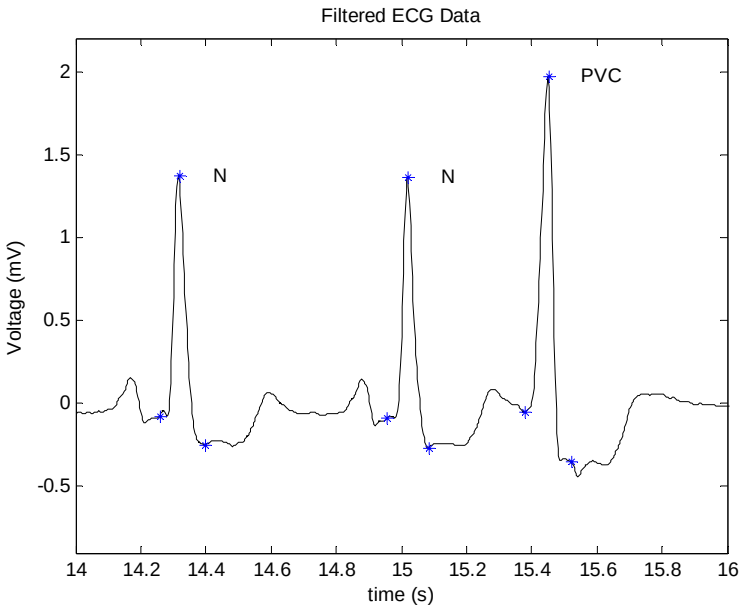

Figure A.3 Filtered ECG signal with Q, R, S points and classification results indicated